European Journal of Medicinal Chemistry 94 (2015) 87–101

Contents lists available at ScienceDirect

European Journal of Medicinal Chemistry

journal homepage: http://www.elsevier.com/locate/ejmech

Original article

Luotonin-A based quinazolinones cause apoptosis and senescence *via* HDAC inhibition and activation of tumor suppressor proteins in HeLa cells

Ramineni Venkatesh [a], M. Janaki Ramaiah [b], Hanmant K. Gaikwad [a], Sridhara Janardhan [c], Rajashaker Bantu [a], Lingaiah Nagarapu [a, *], G. Narahari Sastry [c], A. Raksha Ganesh [b], Manikapal Bhadra [b, *]

[a] Organic Chemistry Division II, CSIR-Indian Institute of Chemical Technology, Tarnaka, Hyderabad 500007, India
[b] Centre for Chemical Biology, CSIR-Indian Institute of Chemical Technology, Tarnaka, Hyderabad 500607, India
[c] Centre for Molecular Modeling, CSIR-Indian Institute of Chemical Technology, Tarnaka, Hyderabad 500607, India

ARTICLE INFO

Article history:
Received 4 September 2014
Received in revised form
6 January 2015
Accepted 28 February 2015
Available online 3 March 2015

Keywords:
Quinazolinone hybrids
Click chemistry
HDACs
Senescence
Docking studies

ABSTRACT

A series of novel quinazolinone hybrids were synthesized by employing click chemistry and evaluated for anti-proliferative activities against MCF-7, HeLa and K562 cell lines. Among these cell lines, HeLa cells were found to respond effectively to these quinazolinone hybrids with IC_{50} values ranging from 5.94 to 16.45 μM. Some of the hybrids (**4q**, **4r**, **4e**, **4k**, **4t**, **4w**) with promising anti-cancer activity were further investigated for their effects on the cell cycle distribution. FACS analysis revealed the G1 cell cycle arrest nature of these hybrids. Further to assess the senescence inducing ability of these compounds, a senescence associated β-gal assay was performed. The senescence inducing nature of these compounds was supported by the effect of hybrid (**4q**) on p16 promoter activity, the marker for senescence. Moreover, cells treated with most effective compound (**4q**) show up-regulation of p53, p21 and down-regulation of HDAC-1, HDAC-2, HDAC-5 and EZH2 mRNA levels. Docking results suggest that, the triazole nitrogen showed Zn^{+2} mediated interactions with the histidine residue of HDACs.

1. Introduction

Cancer is one of the most common diseases worldwide and is the second leading cause of deaths in the world. Drug discovery has played an important role in the development of newer and safer anti-cancer agents that have a broader spectrum of cytotoxicity to tumor cells [1]. Histone deacetylases (HDACs) are important class of enzymes involved in many significant biological functions. They have been linked to a variety of cancers. Altered expression and mutations of genes that encode HDACs have been linked to tumor development as these two factors induce the aberrant transcription of key genes which regulate important cellular functions such as cell proliferation, cell-cycle regulation and apoptosis. HDAC inhibitors have been shown to inhibit cell proliferation by inducing apoptosis and senescence. Thus, HDACs are among the most promising therapeutic targets for cancer treatment [2–4].

Histone deacetylases are functionally a class of enzymes that remove acetyl groups from an ε-N-acetyllysine aminoacid on histone, allowing the histones to wrap the DNA more tightly. HDACs are classified into class I, class II, class III (SIRT proteins) and class IV (HDAC-11). Class I HDAC proteins includes HDAC-1, 2, 3 and 8 whereas class II includes HDAC-4, 5, 6, 7, 9 and both these classes are associated with Zn^{+2} as co-factor [3]. Recent studies have indicated that Histone methyl transferases [HMTs] work along with HDACs and cause epigenetic deregulation that eventually leads to cancer phenotype [5]. Members of HMTs include Enhancer of Zeste Homolog 2 (EZH2), a key component of polycomb repressive complex that catalyzes H3 lysine 27 trimethylation and cause transcriptional gene silencing [6,7]. Recent studies have indicated that EZH2 is a cell regulatory protein that governs senescence and was found to interact with HDAC-1/2 proteins in cancer cells and alter the chromatin structure [8]. Among HDAC inhibitors, SAHA was found to inhibit gall bladder carcinoma [9] and LBH 589 [10–12] was known to inhibit both HDACs and EZH2 in acute leukemia cells. Several HDAC inhibitors (HDACi) are currently under

* Corresponding authors.
E-mail address: lnagarapuiict@yahoo.com (L. Nagarapu).

http://dx.doi.org/10.1016/j.ejmech.2015.02.057
0223-5234/

clinical trials on either monotherapy or combination therapy for cancer treatment [13,14]. HDACi induce different phenotypes in various transformed cells, including growth arrest, activation of the extrinsic and/or intrinsic apoptotic pathways, autophagic cell death, reactive oxygen species (ROS)-induced cell death, mitotic cell death and senescence clearly indicating inhibition of HDACs as a novel promising strategy in human cancer therapy [15,16].

The p53 tumor suppressor is well known to regulate genes that mediate cell cycle arrest, apoptosis, senescence, DNA repair [17]. During tumorigenesis, multiple cooperating genetic events result in inactivation of p53 tumor suppressor pathway, a major regulator of senescence and tumorigenesis [18]. Cellular senescence could be triggered by activation of pathways that are dependent on p53-p21 and p16-pRB with over expression of p16 markedly retarding the growth of HCT-116 cells and evoking the senescent phenotype in cancer cells [19]. Studies have also demonstrated that the HDAC inhibitors such as sodium butyrate and Trichostatin-A are known to induce senescence even in the absence of DNA damage in normal human fibroblast cells that cause tumor cell death [20,21]. Apart from p53, HDAC, the transcriptional repressor EZH2 that belongs to polycomb group is also found to play a critical regulatory role in senescence [22].

The quinazolinone moiety contained in natural products (Luotonin, Rutaecarpine, Tryptanthrin, Chloroqualone, Alloqualone, etc) represents medicinally and pharmaceutically important class of compounds [23,24] because of their diverse range of biological activities such as anti-cancer, diuretic, anti-inflammatory, anti-convulsant and anti-hypertensive [25,26]. In recent years, quinazolinone embedded numerous natural products have been identified [27]. Several other quinazolinone derivatives have been identified with anticancer, mPTP modulators, EGFR and VEGFR-2 inhibitors [28–30]. The cytotoxic alkaloid Luotonin-A (1) and its derivatives infused with quinazolinone moiety are clinically proved as anti-cancer agents (Fig. 1) [31–33].

Luotonin A is a pyrroloquinazolinoquinoline alkaloid extracted from Chinese herbal medicinal plant *Peganum nigellastrum* that functions as human topoisomerase-I poison. Luotonin-A stabilizes the human DNA topoisomerase I-DNA covalent binary complex and mediates topoisomerase-I dependent cytotoxicity in intact cells [34]. Studies [35] have demonstrated that luotonin-A binds to dsDNA through the minor groove and stabilize the topoisomerase I-DNA covalent binary complex and induce DNA cleavage. In view of great potential of Luotonin A, it has been subjected to manipulations (or modifications) for the generation of novel hybrids that have a better potential to cause cytotoxicity as well as target the key proteins that dictates the cell fate such as HDACs and EZH2 in cancer cells.

Current chemotherapy regimens are comprised mostly of single-target drugs which are often plagued by toxic side effects and resistance development. The attractive targets, histone deacetylase (HDAC) and topoisomerase I (Topo I), are cellular modulators that can broadly arrest cancer proliferation through a range of downstream effects. Presently, Researchers are concentrating on agents that can modulate multiple targets that may have superior advantage and fewer side effects over the use of single-target agents. Studies [36,37] have indicated an unanticipated function of Topo I in regulating senescence. In addition, HDAC inhibitors also were found to induce the senescence of corneal myofibroblasts as evidenced by increased staining of beta-galactosidase and upregulated expression of p16 (ink4a) [38].

Studies on pyrroloquinoline nucleus have indicated the potential cytotoxic effects of these chemical compounds on tumor cells [39,40]. As a part of our on-going programme to discover and develop tumor growth inhibitors as well as apoptotic inducers, we have identified several classes of novel potential anti-cancer molecules [41–44]. Here we synthesized novel quinazolinone hybrids of Luotonin A, by employing click chemistry, to elicit combined anti-tumor efficacy/cytotoxicity against different cancer cell lines *in vitro*. The cytotoxicity of these compounds were evaluated on MCF-7 (Human breast cancer), HeLa (human cervical cancer), K562 (human myelogenous leukemia [CML]) cell lines as well as normal HEK (human embryonic kidney cells).

The computational techniques play a vital role in lead molecule identification and its optimization. Both structure based (homology modeling, docking) and ligand based (pharmacophore, QSAR) drug design approaches have been used for the design of better ligands in order to enhance potency, selectivity, pharmacokinetic parameters [45–48]. Hence, in the current study, we have applied both ligand based and structure based techniques on a series of quinazolinone compounds in both EZH2 and HDAC proteins. The crystal structures of HDAC5 and HDAC6 are unknown and hence we have made homology models using human HDAC2 as a template. The site map analysis has been performed on EZH2 structure for the identification of its catalytic domain. The docking studies have been performed to understand the key active site residues of most potent quinazolinone series of compounds in all HDAC, EZH2 proteins and explored all probable binding modes. Ligand based pharmacophore model (AAAHRR) has been built using dataset compounds and

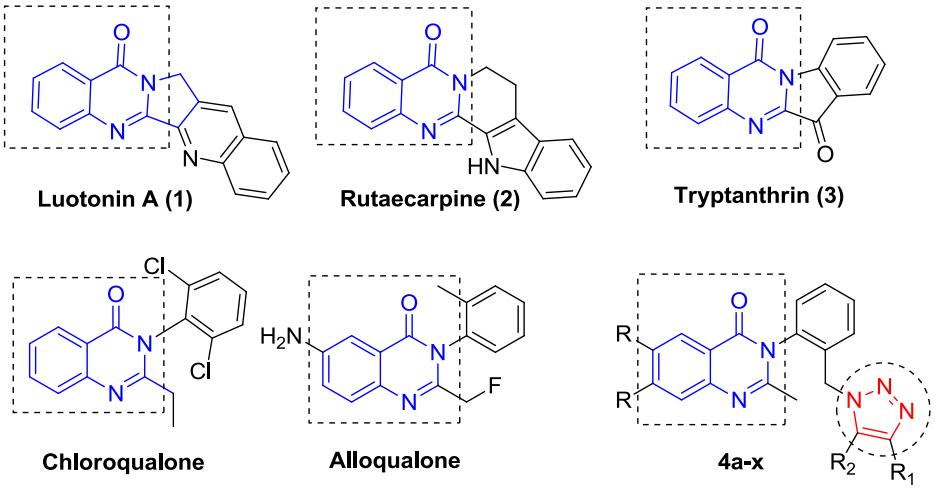

Fig. 1. Quinazolinone scaffold containing natural products and its hybrids (**4a**–**x**).

identified two acceptors, one hydrophobic and two aromatic pharmacophoric features responsible for better ligand binding. The identified structural features from ligand based and structure based approaches could help in rational design of quinazolinone compounds with enhanced potency in EZH2 and HDAC proteins.

2. Results and discussion

2.1. Chemistry

2.1.1. Synthesis of compounds (*8a–b*)

The synthesis of 3-(2-(hydroxymethyl) phenyl)-2-methylquinazolin-4(3*H*)-ones (**8a–b**) was performed in two steps starting from anthranilic acid (**5a–b**) (Scheme 1). The first synthetic step involved in the condensation of anthranilic acid (**5a–b**) with acetic anhydride to afford benzoxazinones (**6a–b**). After evaporation of the excess of anhydride under reduced pressure, the crude product (obtained in quantitative yields) was used without any further purification. Intermediates (**6a–b**) were totally converted into 8a-b, by their treatment with 2-amino benzyl alcohol (**7**), using catalytic amount of TBAB in acetic acid under reflux conditions, in good yields.

2.1.2. Synthesis of quinazolinone hybrids using click chemistry (*4a–r*)

The reaction of 3-(2-(hydroxymethyl)phenyl)-2-methylquinazolin-4(3*H*)-ones (**8a–b**) with tosylchloride and DMAP (catalytic) in dry DCM/pyridine, under N_2 atmosphere at room temperature for 3 h afforded **9a–b**. The reaction between 3-(2-(azidomethyl)phenyl)-2-methylquinazolin-4(3*H*)-ones and various terminal alkynes furnished the corresponding triazoles (**4a–r**). The reagents are commercially available and the reaction completed within 30 min and gave analytically pure products after filtration. Sodium ascorbate reduces the copper (II) sulfate penta hydrate to copper (I), which is active catalyst in this reaction. The presence of copper often results in intensely colored reaction mixture. Scheme 2 demonstrates the procedure's ease and economy, as well as its final reward (Scheme 3).

2.1.3. Synthesis of quinazolinone hybrids (*4s–x*)

The reaction between 3-(2-(hydroxymethyl)phenyl)-2-methylquinazolin-4(3H)-ones (**8a–b**) and different 1,2,3-triazoles by using catalytic amount of *p*TSA in toluene under reflux condition for 36 h produced the corresponding triazoles (**4s–x**).

3. Pharmacology

3.1. In vitro cytotoxicity assay

Novel quinazolinone hybrids (**4a–x**) were evaluated for antiproliferative activity against three different human cancer cell lines i.e., HeLa, MCF-7 and K562 by MTT assay [Table 1]. All the synthesized compounds exhibited significant cytotoxicity when compared to standard drug molecule [Luotonin A]. These molecules exhibited low cytotoxicity in non-cancerous primary cell line HEK. Among the entire series of hybrids, **4q**, **4r**, **4e**, **4k**, **4t** and **4w** have exhibited effective cytotoxicity in the cell lines tested. It is interesting to note that HeLa cells have exhibited stronger cytotoxic response than other cell lines in the study. The hybrids that are unsubstituted at R position exhibited better activity or performance than any other substitution made in the quinazolinone back bone (Table 1). These compounds were further evaluated by employing more precise biological assays to determine the cell cycle as well as tumor suppressive effects. These were found to cause more cytotoxic effects in HeLa and MCF-7 cells which have endogenous wild-type p53 status than K562 with mutation in p53 gene that cause inactivation of p53 [49,50]. Interestingly, these compounds activated p53 expression in cervical cancer cells where in p53 protein is degraded by viral E6 oncoprotein encoded by human papilloma virus. Thus, the presence of wild-type p53 might have possible role in cytotoxic activity by these compounds. Large-scale analysis of cellular response to anticancer drugs typically focuses on variation in potency (half-maximum inhibitory concentration, (IC_{50}), assuming that it is the most important difference between effective and ineffective drugs or sensitive and resistant cells. But recent studies envisaged the importance of considering the parameters other than potency [IC_{50}] to find out drug response [51].

3.2. Cell cycle effects

In order to understand the effect of compounds on cell cycle of treated cells we have conducted flow cytometry experiment following treatment of HeLa cells with effective compounds **4q**, **4r**, **4e**, **4k**, **4t** and **4w** at 4 μM for 48 h and staining with propidium iodide dye. We have observed an irreversible G1 cell cycle arrest in compound **Luotonin A** (75%), **4q** (76%), **4r** (73%), **4e** (72%), **4k** (72%), **4t** (71%), **4w** (71%) treated cells when compared to untreated control cells (62%) (Fig. 2). Increased concentration leads to significant cell death (data is in Supplementary). Interestingly, cells treated with compounds **4q** have exhibited higher percentage of G1 cell cycle arrest when compared to all other tested compounds. These results were in concurrence with the results obtained from cytotoxic assay in cervical cancer cells.

3.3. Compounds induce the senescence phenotype

Cellular senescence is a final common pathway for a number of DNA damage and repair pathways and appears to play a major role in processes such as aging, stress and tumor suppression [52] and is characterized by morphological changes such as blue coloration and adopted a fattened morphology with spread out cytoplasm as observed in senescence associated β-galactosidase (SA-β-gal) staining [53]. Previous studies have indicated that strong irreversible G1 cell cycle arrest might be responsible for senescence phenotype in cancer cells [54,55]. This prompted us to examine senescence as a part of tumor-suppressive mechanism in

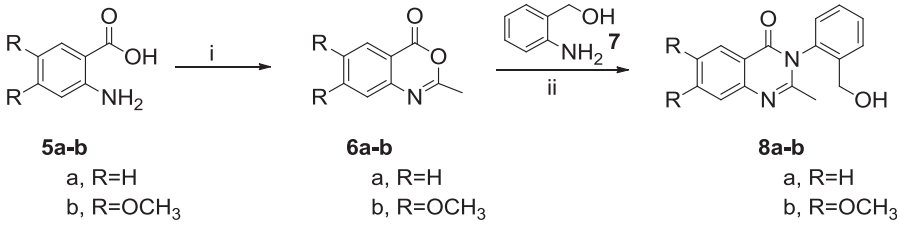

Scheme 1. Synthesis of compounds (**8a–b**): Reagents & conditions: i) Ac_2O, 3 h, reflux, ii) TBAB, AcOH, 120 °C, 1 h, reflux.

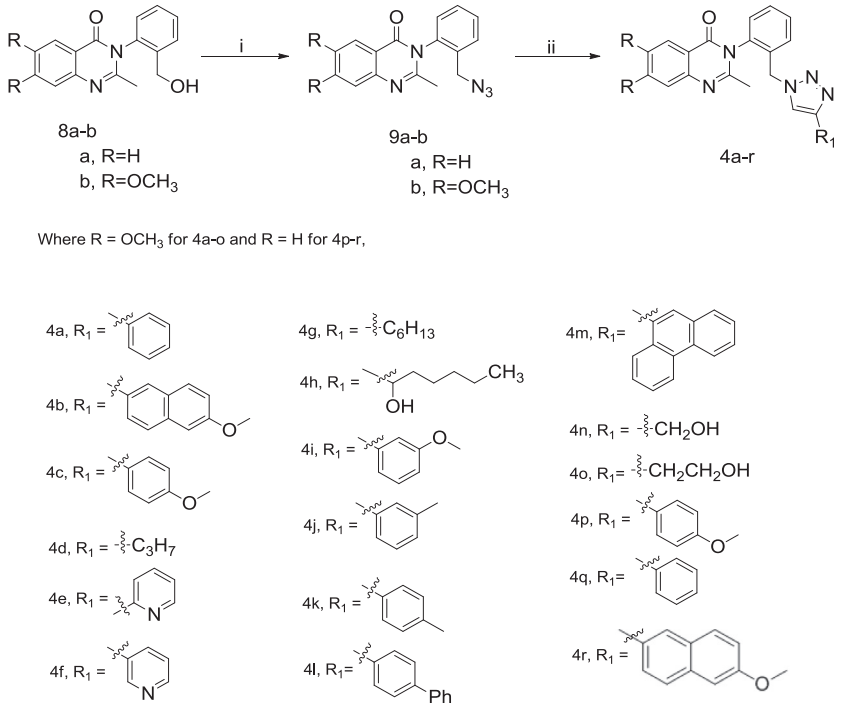

Scheme 2. Synthesis of quinazolinone hybrids using click chemistry (**4a**–**r**): Reagents & conditions: i) a) TsCl, Dry CH_2Cl_2, Py, DMAP, 3 h. b) NaN_3, DMF, 120 °C, 12 h; ii) Substituted acetylenes, $CuSO_4 \cdot 5H_2O$, Sodium ascorbate, THF: H_2O (1:1).

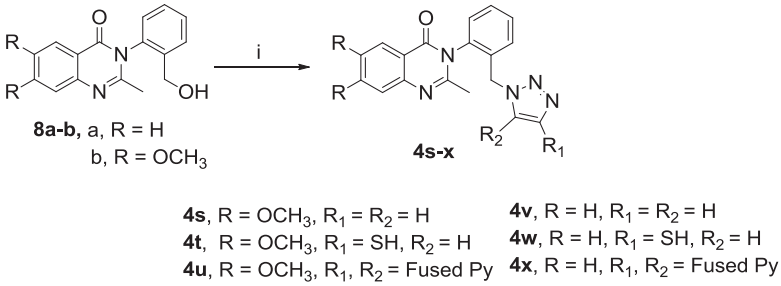

Scheme 3. Synthesis of quinazolinone derivatives (**4s**–**x**): Reagents & conditions: i) Substituted triazoles, *p*TSA, toluene, reflux, 36 h.

compound treated cells [56]. Here we have employed senescence associated β-galactosidase assay to identify senescence [57,58]. Treatment of HeLa cells with Luotonin A, **4q** and Doxorubicin (**Doxo**) for 72 h caused senescence phenotype as observed by enlarged, flattened morphology of cells with enhanced β-gal staining (blue coloration) (Fig. 3).

3.4. Effects on p53 and associated repressive proteins

The p53 tumor suppressor is well known to regulate genes that mediate cell cycle arrest, apoptosis, senescence, DNA repair [17]. Interestingly, cellular senescence may result from a variety of stresses, mainly mediated by two tumor-suppressor pathways involving p53-p21 and p16-pRB [18,19,59]. Moreover, activated p53 is known to suppress EZH2 gene expression by modulating p21 expression [60]. Recent studies have demonstrated that HDAC inhibitors induced the senescence of corneal myofibroblasts as observed by increased staining of β-galactosidase as well as upregulated expression of p16(ink4a) [38].

This prompted us to examine the effect of these compounds on expression of p53, p21, HDACs and EZH2 that play a vital role in controlling cell proliferation via senescence process. HeLa cells were treated with hybrids Doxo, **4q**, Luotonin A by employing gene specific primers against p53, p21, EZH2, HDAC-1, 2 5, 6, 7. We observed an increase in p53, p21 and considerable decrease in expression of EZH2 and HDAC-1, 2 and 5 mRNA levels. Not much change was observed in HDAC-6 and 7 mRNA levels. The effect of compounds on HDAC-1, HDAC-2 mRNA levels was also confirmed by conducting colorimetry based HDAC-1/2 inhibition assay (Fig. 4B). The IC_{50} values for the inhibition of HDAC-1, 2 for **4q** and Luotonin A was derived and was found to be 2.96 and 6.4 μM respectively. Hence, these results clearly indicated that the quinazolinone hybrids show inhibitory effect on HDACs and EZH2 enzymes and by the activation of key tumor suppressor proteins p53 and p21 (Fig. 4). Furthermore, we were interested to examine the involvement of p16 in senescence process by determining its promoter activity. Thus, HeLa cells were treated with **4q**, Doxo, Luotonin A at 4 μM for 48 h and the p16 promoter activity was determined. Results clearly indicated a pronounced increase in p16 promoter activity in compound treated cells. This increased p16 promoter activity is a clear indication of involvement of p16 in the senescence event (Fig. 5).

Table 1
IC_{50} (μM) values of series of Luotonin-A based Quinazolinone compounds obtained from MTT based cytotoxicity assay.[a]

S. No	Compounds	IC_{50} (μM)[a]				Selective Index (SI)[g]		
		MCF-7[b]	HeLa[c]	K562[d]	HEK[e]	MCF-7[h]	HeLa[i]	K562[j]
1	**4a**	9.19	13.71	25.6	64	6.96	4.66	2.5
2	**4b**	18.18	14.62	28.0	68	3.74	4.65	2.42
3	**4c**	13.96	11.88	22.4	72	5.15	6.06	3.2
4	**4d**	14.40	13.25	22.4	74	5.13	5.58	3.3
5	**4e**	18.61	10.57	20.8	252	13.54	23.84	12.11
6	**4f**	10.18	13.25	20.0	54	5.3	4.07	2.7
7	**4g**	17.74	14.62	24.0	53	2.98	3.62	2.2
8	**4h**	17.89	16.0	22.88	48	2.68	3.0	2.09
9	**4i**	15.12	11.88	22.40	51	3.37	4.29	2.27
10	**4j**	18.03	14.4	31.52	56	3.10	3.88	1.77
11	**4k**	14.4	9.92	28.0	204	14.16	20.56	7.28
12	**4l**	10.47	14.17	22.4	71	6.78	5.01	3.16
13	**4m**	13.23	12.8	25.6	89	6.72	6.95	3.47
14	**4n**	15.85	11.88	28.0	110	6.94	9.25	3.92
15	**4o**	14.0	16.0	26.56	124	8.85	7.75	4.66
16	**4p**	14.4	12.8	22.4	116	8.05	9.06	5.17
17	**4q**	8.0	5.94	20.16	256	32	43.09	12.69
18	**4r**	8.72	8.68	19.52	178	20.41	20.50	9.11
19	**4s**	23.70	12.61	28.8	98	4.13	7.77	3.40
20	**4t**	9.77	10.5	30.4	214	21.9	20.38	7.03
21	**4u**	18.56	11.88	19.68	79	4.25	6.64	4.01
22	**4v**	15.27	16.45	22.4	76	4.97	4.62	3.39
23	**4w**	14.98	10.97	26.24	189	12.61	17.22	7.20
24	**Luotonin A**[f]	9.28	5.94	28.8	58	6.25	9.76	2.01

[a] IC_{50} values are indicated as mean ± SD of three independent experiments.
[b] MCF-7, human breast adenocarcinoma cell line.
[c] HeLa, human cervical cancer cell line.
[d] k562, human immortalized mylogenous leukemia cell line.
[e] HEK, human embryonic kidney cell line.
[f] Luotonin A used as a positive control.
[g] Selective Index (SI) for these compounds was deduced as the ratio of IC_{50} of the compound in normal cells over IC_{50} of compound in cancer cells. Selective index (SI) is more for HeLa cells than MCF-7 and K562 cells and thus can be considered as effective in HeLa cells.
[h] Here MCF-7 column depicts the SI index for compounds in MCF-7 cells.
[i] HeLa column represents the SI index for compounds in HeLa cells.
[j] k562, represents the SI index values for the compounds in K562 cells.

4. Molecular modeling studies

In order to understand the probable binding mode of quinazolinone hybrids, molecular docking study was performed with EZH2 and HDACs targets (Fig. 6). The known three dimensional structure of HDAC2 could be utilized for building homology models for unknown structures of HDAC5, HDAC6 to investigate the structural aspects for design of novel selective compounds. The homology models can be used to identify different binding pockets, putative active site residues and binding mode of inhibitors [61,62]. The six featured pharmacophore model (AAAHRR) has been built using a series of 24 quinazolinone compounds. The developed pharmacophore could provide a rational hypothetical picture of the primary chemical features that are responsible for the activity. The pharmacophore modeling and molecular docking studies could provide substantial design clues for the development of novel, potent inhibitors for HDAC target.

4.1. Pharmacophore modeling

In order to identify the essential structural features of the ligand responsible for its potency, we have generated a ligand based pharmacophore model from a dataset comprising of 24 quinazolinone compounds. All possible tautomeric and ionization states of these compounds were considered and subjected to minimization with OPLS-2005 force field, using water as solvent in the GB/SA continuum solvation model. Further, the minimum energy structures were used to conformation generation by employing mixed torsional/low-mode sampling method with default parameters. 4036 conformations thus obtained were used to generate pharmacophore hypotheses. The best common pharmacophore hypothesis AAAHRR has been selected with a *site score* 0.95, *vector score* 0.99 and *volume score* of 0.83 from a set of 86 pharmacophore hypotheses. The identified common pharmacophore hypothesis consists of three acceptors (A), one hydrophobic (H) and two aromatic (R) features. Alignment of the most potent compounds (**4q**, **4t**, **4a**, **4r**) from the dataset molecules using pharmacophore hypothesis (AAAHRR) is shown in Fig. 7.

4.2. Molecular docking

The synthesized quinazolinone series of hybrids showed inhibitory potency on HDACs and EZH2 targets. In order to explore the binding mode and understanding of key active site residues, molecular docking study has been performed. From the docking study, the key active site residues such as (HDAC1: Tyr303, His141; HDAC2: Phe210, His883; HDAC5: Phe901, His610; HDAC7: Phe738, His843; EZH2: Phe557, Cys547) were identified for enhancing its potency. The probable binding mode of most potent compounds (**4q**) in human HDAC1, 2, 5 and EZH2 targets are shown in Fig. 8.

In the present study, the docking result of compound (**4q**) in HDACs and EZH2 proteins are discussed.

4.2.1. HDAC1

The nitrogen of the triazole moiety formed salt bridge (Zn^{+2}) with aspartic acid (Asp126) and histidine residue (His178). The carbonyl moiety of the ligand showed hydrogen bond interaction with histidine residue (His178). The phenyl ring connected to triazole ring shows hydrophobic interactions with Cys151, Met30, Phe150. Another phenyl ring connected between triazole and quinazolinone ring showed π-π interactions with phenylalanine (Phe205, Phe150) residues. Further, the quinazolinone ring showed hydrophobic interactions with Leu271 and its methyl substitution with Phe150 residues.

4.2.2. HDAC2

The carbonyl moiety of quinazolinone ring showed hydrogen bond interaction with histidine (His183) residue. The phenyl ring connected between triazole and quinazolinone ring showed parallel π-π stacking interactions with Phe210. Further, the phenyl ring connected to triazole ring showed hydrophobic interaction with Leu144, Met35 and Cys156. The quinazolinone ring showed hydrophobic interactions with Leu276, Tyr209 and Phe210. The triazole nitrogen showed Zn^{+2} mediated interaction with Asp181 and His183.

4.2.3. HDAC5

The methyl substituted quinazolinone moiety showed interactions with Phe900, Pro972 and Leu973 residues. The phenyl ring between triazole and quinazolinone ring showed parallel π-π stacking interactions with Phe842, Phe901. Another phenyl connected to triazole ring showed hydrophobic interactions with Phe842. The triazole nitrogen showed Zn^{+2} mediated interaction with Asp870, His872.

4.2.4. EZH2

In compound **4q**, the phenyl ring connected to triazole ring showed hydrophobic interaction with Met701, Leu584, Cys580 and Phe557 residues.

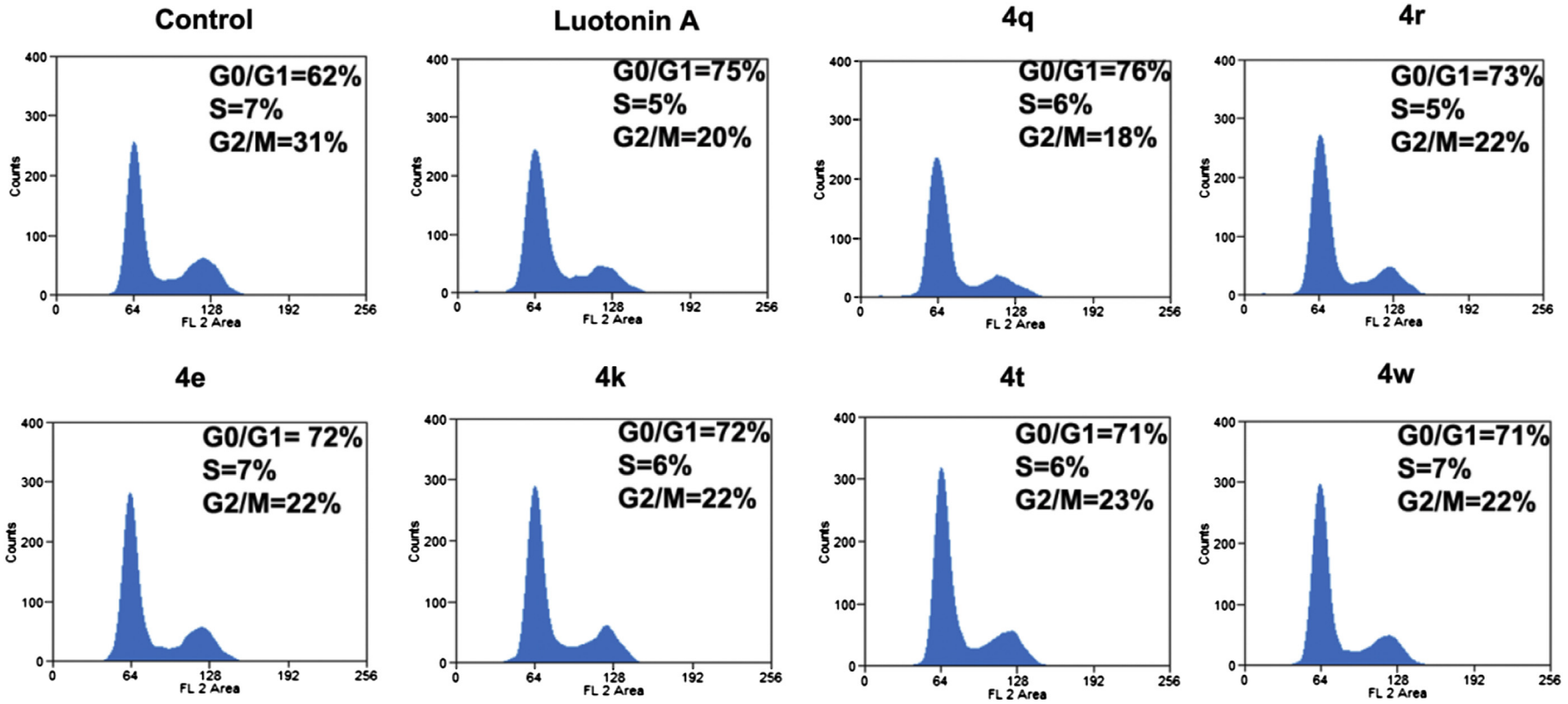

Fig. 2. Cell cycle effects of **4q**, **4r**, **4e**, **4k**, **4t**, **4w** and **Luotonin A** compounds by FACS analysis. HeLa cells were harvested 48 h after treatment with compounds **4q**, **4r**, **4e**, **4k**, **4t**, **4w** and **Luotonin A** at 4 μM. Here untreated cells were used as control. Cell cycle analysis was conducted by staining these cells with propidium iodide as indicated. The percentage of cells accumulated in each phase quantified and represented in the FACS figures.

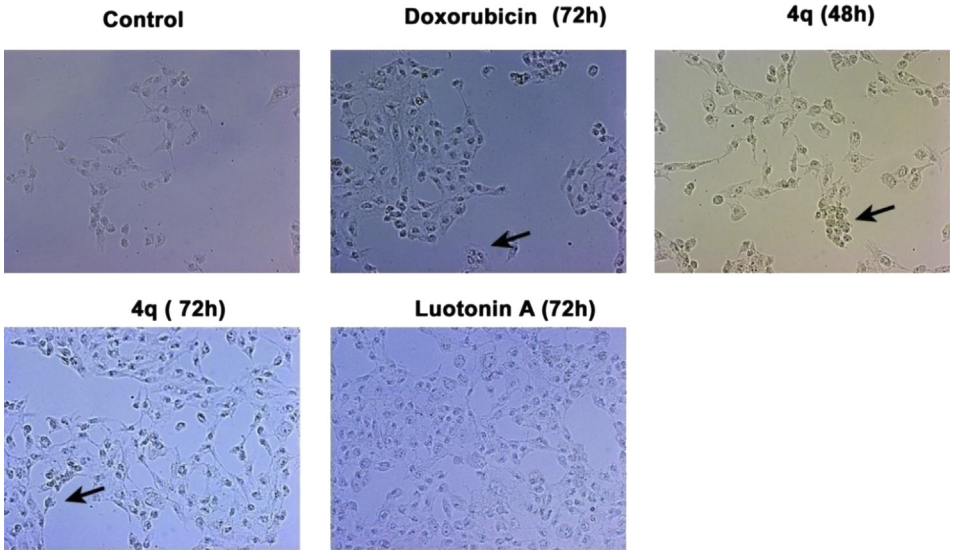

Fig. 3. Quinazolinone hybrids induce cellular senescence in cervical carcinoma [HeLa] cells: Here cells were treated with **Doxo**, **4q**, **Luotonin A** at a concentration of 4 μM for 72 h and senescence associated β-gal assay was conducted using β-galactosidase stain. In this assay senescent cells exhibited enlarged, flattened morphology and turn blue color. **Doxo** was used a positive control and **Luotonin A** was used as standard positive control. (For interpretation of the references to color in this figure legend, the reader is referred to the web version of this article.)

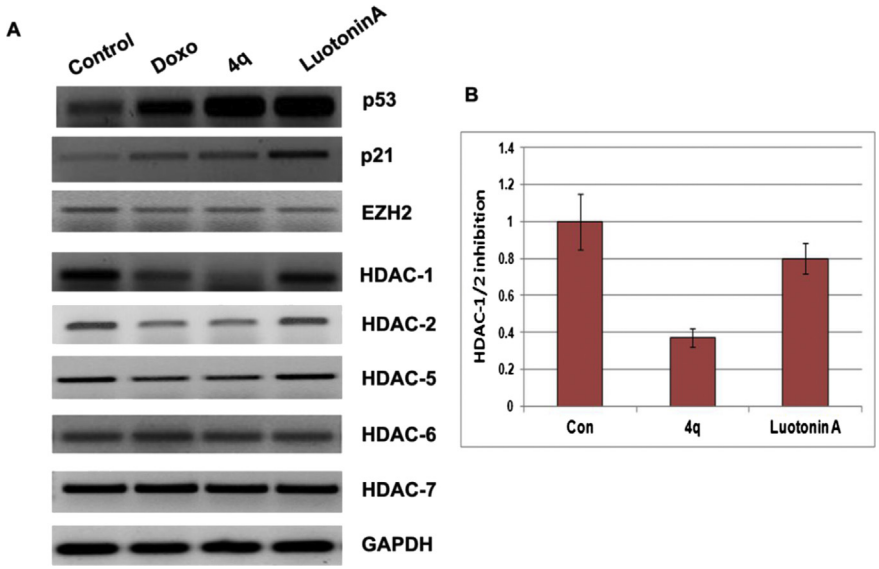

Fig. 4. Quinazolinone hybrids regulate the expression of p53 and repressor complex (HDAC-1, 2, 5, 6, 7 & EZH2) in HeLa cells: HeLa cells were treated with hybrids **Doxo**, **4q**, **Luotonin A** at 4 μM for 48 h. The RNA was isolated and the cDNA prepared was subjected to RT-PCR analysis to study the expression of p53, p21, EZH2, HDAC-1, 2, 5, 6 and 7. [**B**]. HDAC-1, 2 inhibitory activity of compounds was studied by using calorimetry based kit [**Enzo Life Sciences USA**].

In our study, we have explored all the possible binding modes and key active site residues for each compound in all HDACs and EZH2 proteins. Overall docking study revealed that the hydrophobic interactions are more predominant than electrostatic interactions. In all HDACs, the quinazolinone ring was accommodated in the hydrophobic residue region. The substitution of electron-donating group ($-OCH_3$) on quinazolinone ring loses its hydrophobic interactions. The substitution of electron-withdrawing groups on quinazolinone ring might be beneficial in making the ring become more electron deficient, for gaining additional hydrophobic interactions. Also, the substituted phenyl ring connected to triazole ring could be beneficial for enhancing its potency because it accommodated in hydrophobic environment of HDACs (Fig. 8).

5. Conclusion

In conclusion, we developed a novel series of quinazolinone hybrids bearing interesting bioactive triazole scaffold using click chemistry and knowledge-based design combined with molecular modeling techniques, and showed their biological evaluation for anti proliferative activities on cancer cells. All these 24 quinazolinone hybrids (**4a**–**x**) showed significant anti-cancer activity with IC_{50} values ranging from 5.94 μM to 16.45 μM in HeLa cell line. Particularly compound **4q** exhibited higher cytotoxic effects than Luotonin A. Flow-cytometry analysis revealed G1 cell cycle arrest nature of these hybrids. Interestingly, these quinazolinones induced senescence phenotype in HeLa cells. Further, RT-PCR studies proved inhibitory effect of these compounds on

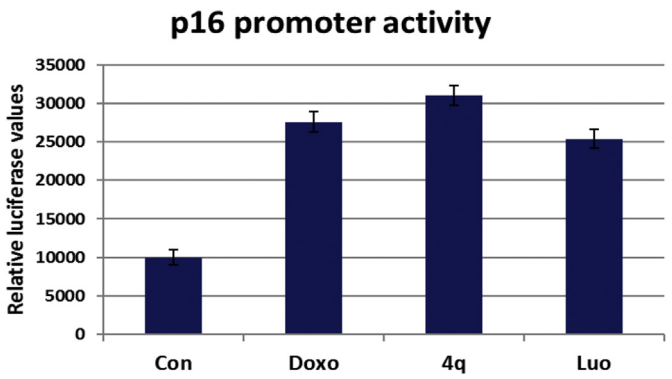

Fig. 5. Effect of quinazolinone hybrids on the p16 promoter activity: HeLa cells were transfected with human p16 promoter and are cloned in a luciferase based pgl3 basic vector followed by treatment with hybrids **Doxo**, **4q**, **Luotonin A** at 4 μM for 48 h. The lysates were subjected to luciferase based luminescence assay. The enhanced p16 promoter activity was observed in hybrid **4q**, **Doxo** and **Luotonin A** treated cells.

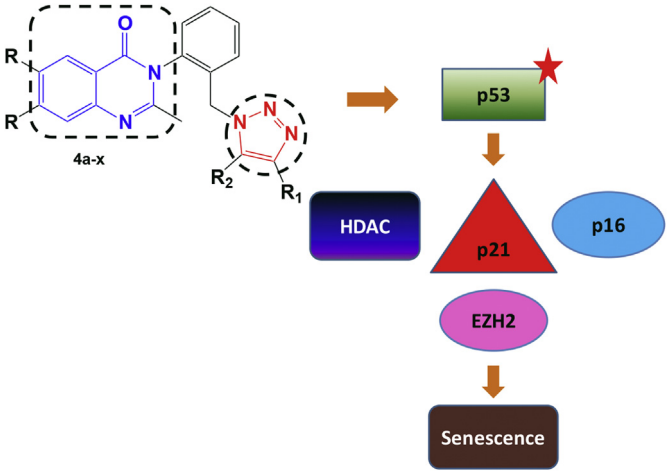

Fig. 6. The graphical picture depicts the molecular mechanism of action of hybrid **4q**. Here hybrids activated p53 and its dependent genes such as p21 and p16. The inhibition of HDACs and the possible activation of p53 and its dependent genes such as p21 and p16 resulted in cell growth arrest and the ultimate result of these expression changes, lead to senescence phenotype.

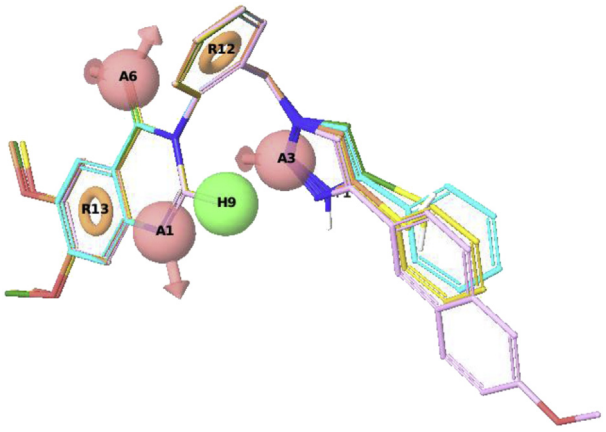

Fig. 7. Alignment of most potent compounds (**4q**, **4t**, **4a**, **4r**) using pharmacophore hypothesis (AAAHRR); A: H-bond acceptor, H: Hydrophobic, R: Aromatic.

HDAC-1, HDAC-2 and EZH2 gene expression. Compound treatment resulted in increase in expression of key tumor suppressor molecules such as p53, p21 as well as p16 promoter activity. The results suggest that the quinazolinone hybrids containing triazole moiety are excellent scaffolds for HDACs and EZH2. The computational techniques such as pharmacophore modeling and molecular docking studies have been applied to support our experimental results. From the docking study we have explored different binding modes and interaction profile of most potent compound (**4q**) in HDACs and EZH2 active sites. The docking study revealed that the nitrogen of triazole moiety shows Zn^{+2} mediated interaction with histidine residue in all HDACs. The substitution of hydrophobic moieties on the core moiety of the inhibitors might be beneficial for enhancing potency. In summary, our results indicate that compound **4q** inhibits HDACs and EZH2 thereby controlling cell cycle progression and proliferation in HeLa cells.

6. Experimental section

6.1. General chemistry

All the chemicals and reagents were purchased from Sigma–Aldrich and SD Fine-Chemicals, Pvt. Ltd. India, and used as received. The reactions were monitored and R_f value was determined using analytical thin layer chromatography (TLC) with Merck Silica gel 60–120 and F_{254} pre-coated plates (0.25 mm thickness). Spot on the TLC plates were visualized using ultraviolet light (254 nm). Flash column chromatography was performed with Merck silica gel (100–200 mesh). Melting points were determined in capillaries and are uncorrected. ^{1}H NMR spectra were recorded on Bruker DRX-300, Varian 400 and Varian-500 NMR spectrometers. ^{13}C NMR spectra were recorded on Bruker DRX-300. Proton chemical shifts are reported in ppm (δ) relative to internal tetramethylsilane (TMS, δ 0.00 or with the solvent reference relative to TMS employed as the internal standard ($CDCl_3$, δ 7.26; DMSO-d_6 δ 2.54) and multiplicities of NMR signals are designated as s (singlet), d (doublet), t (triplet), q (quartet), br (broad), m (multiplet, for unresolved lines). Infrared (IR) spectra were recorded on a Perkin Elmer FT-IR 400 spectrometer; data are reported in wave numbers (cm^{-1}). Mass spectra were recorded on Agilent Technologies 1100 Series (Agilent Chemistation Software). High-resolution mass spectra (HRMS) were obtained by using ESI-QTOF mass spectrometry. All computations and molecular modeling studies have been carried out on Schrodinger software.

6.2. General procedure for the synthesis of compounds (*6a–b*)

A solution of anthranilic acid (10 g, 0.05 mol) in acetic anhydride (19.14 mL, 0.203 mol) was made to react at reflux temperature for 3 h. The excess of solvent was removed by distillation, boiling in the range 125–132 °C at 8 mm/Hg pressure and the residue was obtained as oil that solidified to a white solid. The solid was recrystallized from hexane/pentane to give cyclic compound **6a–b** in the form of long, white, dense needles.

6.2.1. 2-Methyl-4H-benzo[d][1,3]oxazin-4-one (*6a*)

Yield 90%; mp 196–199 °C; IR (KBr) υ in cm^{-1}: 2924, 1683, 1380, 1116, 767; ^{1}H NMR (300 MHz, $CDCl_3$): δ 2.26 (s, 3H, CH_3), 6.66–6.70 (m, 2H, Ar–H), 7.30–7.34 (m, 1H, Ar–H), 7.93 (dd, $J = 1.2$, 6.7 Hz, 1H, Ar–H); ^{13}C NMR (75 MHz, $CDCl_3$): δ 23.9, 114.3, 118.4, 120.8, 129.9, 132.6, 140.1, 167.3, 168.7; ESI MS: $m/z = 162$ $[M+H]^+$; HRMS calculated for $C_9H_7NO_2$: 162.0501, Found: 162.0509.

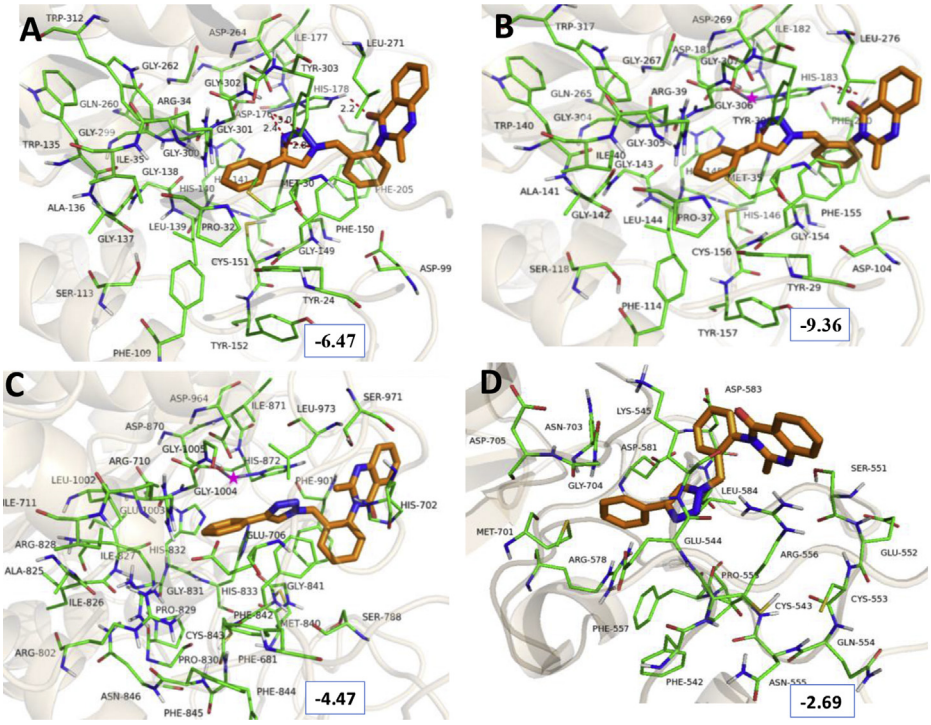

Fig. 8. The probable docked mode of compound **4q** (orange) in the active sites of A: HDAC1, B: HDAC2, C: HDAC5, D: EZH2 the hydrogen bond interactions are shown in red color dotted lines, Zn^{+2} is shown in pink color, the important residues are shown in green color, glide docking score (kcal/mol) in blue box and protein cartoon is represented in wheat color. (For interpretation of the references to color in this figure legend, the reader is referred to the web version of this article.)

*6.2.2. 6,7-Dimethoxy-2-methyl-4H-benzo[d][1,3]oxazin-4-one (**6b**)*

Yield 90%; mp 198–201 °C; IR (KBr) υ in cm^{-1}: 2925, 1667, 1393, 1160, 768; ^1H NMR (300 MHz, $CDCl_3$): δ 2.09 (s, 3H, CH_3), 3.78 (s, 3H, OCH_3), 3.89 (s, 3H, OCH_3), 6.81 (m, 1H, Ar–H), 7.51–7.54 (m, 1H, Ar–H); ^{13}C NMR (75 MHz, $CDCl_3$): δ 23.8, 56.1, 56.3, 106.7, 107.0, 112.4, 143.6, 147.9, 153.1, 155.3, 162.8; ESI MS: $m/z = 222$ $[M+H]^+$; HRMS calculated for $C_{11}H_{11}N0_4$: 222.0701, Found: 222.0695.

*6.3. General procedure for the synthesis of methylquinazolin-4(3H)-ones (**8a–b**)*

To a stirred solution of compound **6a–b** (8.0 g, 0.036 mol) and compound **7** (4.45 g, 0.036 mol) in acetic acid (50 mL), tetra-*n*-butyl ammonium bromide (2 mol%) was added at room temperature. After heating at reflux temperature for 1 h, the reaction mixture was cooled to rt and neutralized with saturated $NaHCO_3$ solution (20 mL). $CHCl_3$ (100 mL) was added to the mixture. The organic layer was separated, dried with Na_2SO_4 and concentrated under reduced pressure to obtain a residue that was purified by column chromatography over silica gel (6:4, ethyl acetate/hexane) to afford **8a–b** as white solid.

*6.3.1. 3-(2-(Hydroxyl methyl)phenyl)-2-methylquinazolin-4(3H)-one (**8a**)*

Yield 62%; mp 186–189 °C; IR (KBr) υ in cm^{-1}: 2924, 1683, 1596, 1380, 1267, 1116, 767; ^1H NMR (300 MHz, $CDCl_3$): δ 2.15 (s, 3H, CH_3), 4.36 (s, 2H, CH_2), 6.96–7.03 (m, 1H, Ar–H), 7.06–7.14 (m, 1H, Ar–H), 7.41–7.51 (m, 2H, Ar–H), 7.60–7.67 (m, 1H, Ar–H), 7.74 (t, $J = 7.6$, 15.3 Hz, 1H, Ar–H), 7.92 (d, $J = 7.6$ Hz, 1H, Ar–H), 8.18 (d, $J = 7.6$ Hz, 1H, Ar–H); ^{13}C NMR (75 MHz, $CDCl_3$): δ 23.9, 60.9, 122.4, 124.2, 126.6, 126.7, 126.9, 127.9, 128.7, 129.3, 129.9, 130.1, 134.8, 137.8, 154.4, 162.5; ESI MS: $m/z = 267$ $[M+H]^+$; HRMS calculated for $C_{16}H_{14}N_20_2$: 267.1100, Found: 267.1108.

*6.3.2. 3-(2-(Hydroxymethyl)phenyl)-6,7-dimethoxy-2-methylquinazolin-4(3H)-one (**8b**)*

Yield 62%; mp 191–194 °C; IR (KBr) υ in cm^{-1}: 2936, 1668, 1505, 1394, 1252, 1028, 753; ^1H NMR (300 MHz, $CDCl_3$): δ 2.17 (s, 3H, CH_3), 4.38 (s, 6H, OCH_3), 4.60 (s, 2H, CH_2), 7.13 (d, $J = 7.6$ Hz, 1H, Ar–H), 7.40–7.57 (m, 1H, Ar–H), 7.62–7.72 (m, 1H, Ar–H), 7.75 (t, $J = 7.6$, 15.3 Hz, 1H, Ar–H), 7.93 (d, $J = 7.6$ Hz, 1H, Ar–H), 8.20 (d, $J = 7.6$ Hz, 1H, Ar–H); ^{13}C NMR (75 MHz, $CDCl_3$): δ 23.8, 56.1, 56.2, 61.1, 105.7, 107.0, 113.4, 128.1, 129.3, 129.9, 130.4, 136.0, 137.9, 143.6, 148.9, 153.1, 155.3, 161.8; ESI MS: $m/z = 327$ $[M+H]^+$; HRMS calculated for $C_{18}H_{18}N_20_4$: 327.1300, Found: 327.1295.

*6.4. General procedure for the synthesis of compounds (**9a–b**)*

A suspension of compound **8a–b** (6g, 0.0184 mol), TsCl (4.207 g, 0.022 mol), pyridine (17 mL), and a catalytic amount of DMAP in dry CH_2Cl_2 (80 mL) was stirred under N_2 atmosphere at rt for 3 h. After completion of reaction as indicated by the TLC, water (20 mL) was added to the reaction mixture. The organic layer was washed with water (3 x 20 mL). The CH_2Cl_2 layer was separated, dried with Na_2SO_4 and concentrated under *vacuum*. The obtained residue (tosylated) was dissolved in DMF (100 mL), NaN_3 (3.589 g, 0.055 mol) was added and the reaction mixture was heated at 120 °C for 12 h. After completion of the reaction (monitored by TLC), the reaction mixture was brought to rt and added diethyl ether (100 mL). The organic layer was washed with cold water (3 x 50 mL), separated, dried with Na_2SO_4 and concentrated under *vacuum*. Following compound **9a–b** was obtained by column chromatography over silica gel (7:3, ethyl acetate/hexane).

*6.4.1. 3-(2-(Azidomethyl)phenyl)-2-methylquinazolin-4(3H)-one (**9a**)*

Yield 67%; mp 188–191 °C; IR (KBr) υ in cm^{-1}: 2917, 1621, 1380, 1219, 1020, 771; ^1H NMR (300 MHz, $CDCl_3$): δ 2.21 (s, 3H, CH_3), 4.16

(d, $J = 14.1$ Hz, $1H_a$, CH_2), 4.27 (d, $J = 14.1$ Hz, $1H_b$, CH_2), 7.12 (s, 1H, Ar–H), 7.22–7.25 (m, 1H, Ar–H), 7.53–7.56 (m, 2H, Ar–H), 7.56–7.60 (m, 2H, Ar–H), 7.74–7.80 (d, $J = 8.0$ Hz, 1H, Ar–H), 8.12 (d, $J = 9.0$ Hz, 1H, Ar–H); ^{13}C NMR (125 MHz, $CDCl_3$): δ 23.9, 51.0, 105.8, 107.3, 113.5, 128.7, 129.8, 129.9, 130.2, 133.2, 136.6, 143.8, 148.9, 152.7, 155.2, 161.0; ESI MS: $m/z = 292$ $[M+H]^+$; HRMS calculated for $C_{16}H_{13}N_50$: 292.1500, Found: 292.1509.

6.4.2. 3-(2-(Azidomethyl)phenyl)-6,7-dimethoxy-2-methylquinazolin-4(3H)-one (**9b**)

Yield 67%; mp 195–198 °C; IR (KBr) υ in cm^{-1}: 2940, 1668, 1506, 1394, 1252, 1028, 758; ^1H NMR (300 MHz, $CDCl_3$): δ 2.21 (s, 3H, CH_3), 3.99 (s, 3H, OCH_3), 4.02 (s, 3H, OCH_3), 4.18 (d, $J = 14.1$ Hz, $1H_a$, CH_2), 4.31 (d, $J = 14.1$ Hz, $1H_b$, CH_2), 7.12 (s, 1H, Ar–H), 7.22–7.25 (m, 1H, Ar–H), 7.53–7.56 (m, 2H, Ar–H), 7.56–7.60 (m, 2H, Ar–H); ^{13}C NMR (125 MHz, $CDCl_3$): δ 23.9, 51.0, 56.2, 56.2, 105.8, 107.3, 113.5, 128.7, 129.8, 129.9, 130.2, 133.2, 136.6, 143.8, 148.9, 152.7, 155.2, 161.0; ESI MS: $m/z = 352$ $[M+H]^+$; HRMS calculated for $C_{18}H_{17}N_50_3$: 352.1500, Found: 352.1509.

6.5. General procedure for the synthesis of compounds (**4a**–**r**)

To a suspension of hetero aryl azide **9a**–**b** (100 mg, 0.284 mol) and alkynes (0.284 mol) in THF: water (1:1) (10 mL), $CuSO_4.5H_2O$ (5 mol%) and sodium ascorbate (10 mol%) were added. The reaction mixture was stirred at rt for 30 min. After completion of the reaction, as indicated by TLC, the reaction mixture was diluted with water (10 mL) and extracted with ethyl acetate (3 x 10 mL). The ethyl acetate extracts were combined, dried with Na_2SO_4 and evaporated to dryness under reduced pressure. The obtained crude product was purified by flash column chromatography over silica gel (5:95, methanol/ethyl acetate) to afford compounds **4a**–**r**.

6.5.1. 6,7-Dimethoxy-2-methyl-3-(2-((4-phenyl-1H-1,2,3-triazol-1yl)methyl)phenyl)quinazolin-4(3H)-one (**4a**)

Yield 85%; mp 98–101 °C; IR (KBr) υ in cm^{-1}: 2925, 2853, 1667, 1505, 1393, 1248, 1160, 768; ^1H NMR (300 MHz, $CDCl_3$): δ 2.09 (s, 3H, CH_3), 4.00 (s, 3H, OCH_3), 4.02 (s, 3H, OCH_3), 5.30 (d, $J = 15.1$ Hz, $1H_a$, CH_2), 5.56 (d, $J = 15.1$ Hz, $1H_b$, CH_2), 7.10 (s, 1H, Ar–H), 7.36–7.43 (m, 5H, Ar–H), 7.52–7.57 (m, 1H, Ar–H), 7.59 (s, 1H, Ar–H), 7.69 (s, 1H, Ar–H), 7.73–7.77 (m, 1H, Ar–H), 7.78–7.83 (m, 1H, Ar–H), 7.89–7.93 (m, 1H, Ar–H); ^{13}C NMR (75 MHz, $CDCl_3$): δ 23.8, 49.9, 55.8, 56.3, 105.7, 107.5, 109.0, 113.6, 120.3, 123.7, 125.7, 127.6, 128.1, 128.7, 128.8, 129.3, 129.7, 129.9, 130.0, 130.3, 134.5, 137.9, 143.9, 149.1, 155.5; ESI MS: $m/z = 454$ $[M+H]^+$; HRMS calculated for $C_{26}H_{24}0_3N_5$: 454.1873, Found: 454.1862.

6.5.2. 6,7-Dimethoxy-3-(2-((4-(6-methoxynaphthalen-2-yl)-1H-1,2,3-triazol-1-yl)methyl)phenyl)-2-methylquinazolin-4(3H)-one (**4b**)

Yield 85%; mp 188–191 °C; IR (KBr) υ in cm^{-1}: 3010, 2936, 2840, 1668, 1505, 1394, 1252, 1028, 753; ^1H NMR (300 MHz, $CDCl_3$): δ 2.27 (s, 3H, CH_3), 3.96 (s, 3H, OCH_3), 3.98 (s, 3H, OCH_3), 4.01 (s, 3H, OCH_3), 5.55 (d, $J = 15.1$ Hz, $1H_a$, CH_2), 5.81 (d, $J = 15.1$ Hz, $1H_b$, CH_2), 6.73–6.80 (m, 2H, Ar–H), 6.81–6.86 (m, 1H, Ar–H), 6.94–7.06 (m, 1H, Ar–H), 7.06–7.15 (m, 2H, Ar–H), 7.53–7.57 (m, 1H, Ar–H), 7.59 (bs, 2H, Ar–H), 7.68–7.77 (m, 1H, Ar–H), 7.80–7.99 (m, 1H, Ar–H), 8.09–8.13 (m, 1H, Ar–H), 8.22 (bs, 1H, Ar–H); ^{13}C NMR (75 MHz, $CDCl_3$): δ 23.6, 50.1, 55.2, 56.2, 56.3, 105.7, 105.8, 107.4, 113.4, 119.1, 120.3, 124.3, 125.4, 128.1, 127.1, 128.4, 128.8, 128.9, 129.6, 130.2, 130.3, 131.9, 132.9, 134.3, 136.3, 143.7, 148.2, 149.2, 152.6, 155.5, 157.9, 161.2. ESI MS: $m/z = 534$ $[M+H]^+$; HRMS calculated for $C_{31}H_{28}0_4N_5$: 534.2135, Found: 534.2128.

6.5.3. 6,7-Dimethoxy-3-(2-((4-(4-methoxyphenyl)-1H-1,2,3-triazol-1-yl)methyl)phenyl)-2-methyl quinazolin-4(3H)-one (**4c**)

Yield 85%; mp 182–185 °C; IR (KBr) υ in cm^{-1}: 2927, 1668, 1506, 1394, 1219, 1025, 772; ^1H NMR (300 MHz, $CDCl_3$): δ 2.27 (s, 3H, CH_3), 3.96 (s, 3H, OCH_3), 3.99 (s, 3H, OCH_3), 4.02 (s, 3H, OCH_3), 5.28 (d, $J = 15.1$ Hz, $1H_a$, CH_2), 5.54 (d, $J = 15.1$ Hz, $1H_b$, CH_2), 6.76 (d, $J = 2.2$ Hz, 1H, Ar–H), 6.82 (d, $J = 3.0$ Hz, 1H, Ar–H), 6.85 (d, $J = 2.2$ Hz, 1H, Ar–H), 6.93 (d, $J = 8.3$ Hz, 1H, Ar–H), 6.99 (s, 1H, Ar–H), 7.02 (s, 1H, Ar–H), 7.12 (s, 1H, Ar–H), 7.37–7.42 (m, 1H, Ar–H), 7.52–7.56 (m, 1H, Ar–H), 7.59 (s, 1H, Ar–H), 7.67 (d, $J = 9.0$ Hz, 1H, Ar–H); ^{13}C NMR (75 MHz, $CDCl_3$): δ 23.9, 49.9, 55.2, 56.0, 56.2, 105.9, 107.2, 107.5, 111.0, 111.5, 113.4, 113.9, 114.0, 119.5, 120.1, 127.0, 128.9, 130.0, 130.2, 130.6, 143.6, 148.8, 149.4, 149.9, 153.3, 155.1, 161.8; ESI MS: $m/z = 484$ $[M+H]^+$; HRMS calculated for $C_{27}H_{26}0_4N_5$: 484.1979, Found: 484.1974.

6.5.4. 6,7-Dimethoxy-2-methyl-3-(2-((4-propyl-1H-1,2,3-triazol-1-yl)methyl)phenyl)quinazolin-4(3H)-one (**4d**)

Yield 85%; mp 146–149 °C; IR (KBr) υ in cm^{-1}: 2927, 1668, 1394, 1219, 1025, 772; ^1H NMR (300 MHz, $CDCl_3$): δ 0.90 (s, 3H, CH_3), 1.61 (t, $J = 7.1$, 14.1 Hz, 2H, CH_2), 2.07 (s, 3H, CH_3), 2.60 (t, $J = 7.3$, 15.1 Hz, 2H, CH_2), 3.98 (s, 3H, OCH_3), 4.01 (s, 3H, OCH_3), 5.28 (d, $J = 15.2$ Hz, $1H_a$, CH_2), 5.54 (d, $J = 15.2$ Hz, $1H_b$, CH_2), 7.11 (s, 1H, Ar–H), 7.17–7.28 (m, 2H, Ar–H), 7.36–7.42 (m, 1H, Ar–H), 7.50–7.56 (m, 1H, Ar–H), 7.58 (s, 1H, Ar–H), 7.64 (d, $J = 8.3$ Hz, 1H, Ar–H); ^{13}C NMR (75 MHz, $CDCl_3$): δ 13.7, 22.7, 23.7, 31.0, 35.5, 49.8, 56.3, 105.7, 107.3, 113.6, 120.0, 125.6, 128.7, 130.2, 132.9, 136.2, 143.0, 143.9, 148.0, 149.1, 152.4, 155.5, 161.1; ESI MS: $m/z = 420$ $[M+H]^+$; HRMS calculated for $C_{23}H_{26}N_50_3$: 420.1957, Found: 420.1896.

6.5.5. 6,7-Dimethoxy-2-methyl-3-(2-((4-(pyridin-2-yl)-1H-1,2,3-triazol-1-yl) methyl) phenyl) quinazolin-4(3H)-one (**4e**)

Yield 85%; mp 180–183 °C; IR (KBr) υ in cm^{-1}: 2928, 1668, 1506, 1395, 1219, 1029, 776; ^1H NMR (300 MHz, $CDCl_3$): δ 2.08 (s, 3H, CH_3), 4.02 (s, 6H, $2OCH_3$), 4.96 (dd, $J = 5.6$, 15.3 Hz, 2H, CH_2), 6.61 (d, $J = 6.9$ Hz, 1H, Ar–H), 7.01–7.08 (m, 1H, Ar–H), 7.12 (s, 1H, Ar–H), 7.29 (s, 1H, Ar–H), 7.37 (d, $J = 4.5$ Hz, 1H, Ar–H), 7.41–7.70 (m, 4H, Ar–H); ^{13}C NMR (75 MHz, $CDCl_3$): δ 29.6, 31.5, 56.3, 105.8, 107.5, 113.4, 114.0, 115.7, 123.3, 123.8, 128.8, 130.2, 135.1, 142.3, 143.8, 149.1, 152.5, 155.4, 159.2, 159.9, 161.2; ESI MS: $m/z = 455$ $[M+H]^+$; HRMS calculated for $C_{25}H_{23}N_60_3$: 455.1753, Found: 455.1813.

6.5.6. 6,7-Dimethoxy-2-methyl-3-(2-((4-(pyridin-3-yl)-1H-1,2,3-triazol-1-yl) methyl) phenyl) quinazolin-4-(3H)-one (**4f**)

Yield 85%; mp 100–103 °C; IR (KBr) υ in cm^{-1}: 2928, 1670, 1506, 1395, 1219, 1029, 776; ^1H NMR (300 MHz, $CDCl_3$): δ 2.08 (s, 3H, CH_3), 4.00 (s, 3H, OCH_3), 4.03 (s, 3H, OCH_3), 5.31 (d, $J = 15.1$ Hz, $1H_a$, CH_2), 5.60 (d, $J = 15.1$ Hz, $1H_b$, CH_2), 7.11 (s, 1H, Ar–H), 7.25 (s, 1H, Ar–H), 7.41–7.47 (m, 2H, Ar–H), 7.52 (s, 1H, Ar–H), 7.53–7.64 (m, 4H, Ar–H), 7.84 (s, 1H, Ar–H), 8.16 (d, $J = 7.5$ Hz, 1H, Ar–H); ^{13}C NMR (75 MHz, $CDCl_3$): δ 29.6, 50.0, 56.3, 56.3, 102.0, 103.5, 105.7, 107.5, 113.3, 120.8, 121.9, 129.0, 130.1, 130.3, 130.5, 131.7, 132.6, 136.5, 143.9, 145.0, 147.0, 149.3, 152.4, 155.6, 161.3; ESI MS: $m/z = 455$ $[M+H]^+$; HRMS calculated for $C_{25}H_{23}N_6O_3$: 455.1753, Found: 455.1809.

6.5.7. 3-(2-((4-Hexyl-1H-1,2,3-triazol-1-yl)methyl)phenyl)-6,7-dimethoxy-2-methylquinazolin-4(3H)-one (**4g**)

Yield 85%; mp 160–163 °C; IR (KBr) υ in cm^{-1}: 2928, 1685, 1470, 1378, 1276, 1126, 772; ^1H NMR (300 MHz, $CDCl_3$): δ 0.82–0.96 (m, 6H, $3CH_2$), 1.55 (t, $J = 7.3$, 14.7 Hz, 3H, CH_3), 2.02 (s, 3H, CH_3), 2.61 (t, $J = 7.3$, 15.1 Hz, 2H, CH_2), 4.01 (s, 3H, OCH_3), 4.03 (s, 3H, OCH_3), 5.20 (d, $J = 15.2$ Hz, $1H_a$, CH_2), 5.46 (d, $J = 15.2$ Hz, $1H_b$, CH_2), 7.13 (s, 1H, Ar–H), 7.18–7.25 (m, 2H, Ar–H), 7.31–7.36 (bs, 1H, Ar–H), 7.49–7.56 (m, 2H, Ar–H), 7.59 (s, 1H, Ar–H); ^{13}C NMR (75 MHz,

$CDCl_3$): δ 13.7, 22.2, 23.7, 25.2, 29.3, 29.6, 31.3, 49.8, 56.2, 56.3, 105.8, 107.5, 113.4, 128.7, 129.0, 130.0, 130.2, 133.1, 136.3, 143.9, 149.1, 152.5, 155.5, 161.2; ESI MS: $m/z = 462$ $[M+H]^+$; HRMS calculated for $C_{26}H_{32}N_5O_3$: 462.2427, Found: 462.2409.

*6.5.8. 3-(2-((4-(1-Hydroxyhexyl)-1H-1,2,3-triazol-1-yl)methyl) phenyl)-6,7-dimethoxy-2-methyl quinazolin-4(3H)-one (**4h**)*

Yield 85%; mp 155–158 °C; IR (KBr) υ in cm^{-1}: 2928, 1684, 1471, 1378, 1276, 1126, 776; ^1H NMR (300 MHz, $CDCl_3$): δ 0.87 (s, 3H, CH_3), 1.27 (s, 6H, $3CH_2$), 1.71–1.91 (bs, 2H, CH_2), 1.98 (d, $J = 8.1$ Hz, 3H, CH_3), 4.01 (s, 3H, OCH_3), 4.03 (s, 3H, OCH_3), 4.73–4.97 (bs, 1H, CH), 5.24 (d, $J = 15.2$ Hz, $1H_a$, CH_2), 5.48 (d, $J = 15.2$ Hz, $1H_b$, CH_2), 7.11 (s, 1H, Ar–H), 7.19–7.25 (m, 1H, Ar–H), 7.34–7.45 (bs, 2H, Ar–H), 7.50–7.56 (bs, 2H, Ar–H), 7.59 (s, 1H, Ar–H); ^{13}C NMR (75 MHz, $CDCl_3$): δ 13.9, 22.5, 23.6, 23.7, 25.0, 25.1, 29.6, 31.5, 31.5, 56.2, 56.3, 105.8, 107.4, 113.4, 113.4, 128.8, 130.2, 130.3, 132.8, 136.4, 143.8, 143.8, 149.1, 152.5, 152.6, 155.5, 161.1; ESI MS: $m/z = 478$ $[M+H]^+$; HRMS calculated for $C_{26}H_{32}N_5O_4$: 478.2376, Found: 478.2429.

*6.5.9. 6,7-Dimethoxy-3-(2-((4-(3-methoxyphenyl)-1H-1,2,3-triazol-1-yl)methyl)phenyl)-2-methyl quinazolin-4(3H)-one (**4i**)*

Yield 85%; mp 88–91 °C; IR (KBr) υ in cm^{-1}: 2927, 1666, 1506, 1394, 1219, 1025, 772; ^1H NMR (300 MHz, $CDCl_3$): δ 2.06 (s, 3H, CH_3), 3.84 (s, 3H, OCH_3), 3.98 (s, 3H, OCH_3), 4.01 (s, 3H, OCH_3), 5.29 (d, $J = 15.1$ Hz, $1H_a$, CH_2), 5.54 (d, $J = 15.1$ Hz, $1H_b$, CH_2), 6.83–6.89 (m, 1H, Ar–H), 7.12 (s, 1H, Ar–H), 7.29 (s, 1H, Ar–H), 7.34–7.42 (m, 3H, Ar–H), 7.50–7.55 (m, 3H, Ar–H), 7.58 (s, 1H, Ar–H), 7.69 (s, 1H, Ar–H); ^{13}C NMR (75 MHz, $CDCl_3$): δ 29.5, 49.9, 55.2, 56.1, 56.2, 105.7, 107.4, 110.7, 113.3, 114.1, 118.0, 120.5, 128.8, 129.6, 130.0, 130.1, 130.2, 131.5, 132.8, 136.3, 143.8, 147.8, 149.0, 152.4, 155.4, 159.8, 161.1; ESI MS: $m/z = 484$ $[M+H]^+$; HRMS calculated for $C_{27}H_{26}N_5O_4$: 484.1907, Found: 484.1961.

*6.5.10. 6,7-Dimethoxy-2-methyl-3-(2-((4-(m-tolyl)-1H-1,2,3-triazol-1-yl) methyl) phenyl) quinazolin-4(3H)-one (**4j**)*

Yield 85%; mp 87–90 °C; IR (KBr) υ in cm^{-1}: 2922, 1669, 1509, 1394, 1219, 1025, 778; ^1H NMR (300 MHz, $CDCl_3$): δ 2.06 (s, 3H, CH_3), 2.38 (s, 3H, CH_3), 4.00 (s, 3H, OCH_3), 4.02 (s, 3H, OCH_3), 5.30 (d, $J = 15.4$ Hz, $1H_a$, CH_2), 5.56 (d, $J = 15.4$ Hz, $1H_b$, CH_2), 7.08–7.16 (m, 2H, Ar–H), 7.30 (s, 1H, Ar–H), 7.36–7.42 (m, 1H, Ar–H), 7.48–7.57 (m, 4H, Ar–H), 7.59 (s, 2H, Ar–H), 7.67 (s, 1H, Ar–H); ^{13}C NMR (75 MHz, $CDCl_3$): δ 19.1, 29.6, 56.2, 56.2, 71.7, 105.8, 107.5, 113.4, 120.3, 122.8, 126.3, 128.5, 128.7, 128.9, 130.1, 130.2, 130.8, 132.3, 132.9, 136.3, 138.3, 143.9, 149.1, 152.4, 155.4, 161.2, 167.7; ESI MS: $m/z = 468$ $[M+H]^+$; HRMS calculated for $C_{27}H_{26}N_5O_3$: 468.1957, Found: 468.2021.

*6.5.11. 6,7-Dimethoxy-2-methyl-3-(2-((4-(p-tolyl)-1H-1,2,3-triazol-1-yl)methyl)phenyl)quinazolin-4(3H)-one (**4k**)*

Yield 85%; mp 170–173 °C; IR (KBr) υ in cm^{-1}: 2922, 1668, 1509, 1394, 1218, 1025, 778; ^1H NMR (300 MHz, $CDCl_3$): δ 2.09 (s, 3H, CH_3), 2.38 (s, 3H, CH_3), 4.01 (s, 3H, OCH_3), 4.04 (s, 3H, OCH_3), 5.30 (d, $J = 15.4$ Hz, $1H_a$, CH_2), 5.56 (d, $J = 15.4$ Hz, $1H_b$, CH_2), 7.11 (s, 1H, Ar–H), 7.22 (d, $J = 7.7$ Hz, 1H, Ar–H), 7.37–7.43 (m, 1H, Ar–H), 7.53–7.58 (m, 4H, Ar–H), 7.61 (s, 1H, Ar–H), 7.65 (d, $J = 8.8$ Hz, 1H, Ar–H), 7.73–7.77 (m, 2H, Ar–H); ^{13}C NMR (75 MHz, $CDCl_3$): δ 19.0, 29.6, 56.2, 56.2, 71.7, 105.7, 107.5, 113.7, 120.0, 124.1, 125.5, 128.7, 129.3, 130.0, 130.2, 130.8, 132.2, 132.9, 136.2, 137.9, 143.8, 148.0, 149.0, 152.4, 155.4, 161.1, 167.5; ESI MS: $m/z = 468$ $[M+H]^+$; HRMS calculated for $C_{27}H_{26}N_5O_3$: 468.1957, Found: 468.2019.

*6.5.12. 3-(2-((4-([1,1′-Biphenyl]-4-yl)-1H-1,2,3-triazol-1-yl) methyl)phenyl)-6,7-dimethoxy-2-methyl quinazolin-4(3H)-one (**4l**)*

Yield 85%; mp 80–83 °C; IR (KBr) υ in cm^{-1}: 3010, 2939, 2841, 1668, 1500, 1395, 1259, 1028, 759; ^1H NMR (300 MHz, $CDCl_3$): δ 2.08 (s, 3H, CH_3), 3.98 (s, 3H, OCH_3), 4.00 (s, 3H, OCH_3), 5.31 (d, $J = 15.8$ Hz, $1H_a$, CH_2), 5.57 (d, $J = 15.8$ Hz, $1H_b$, CH_2), 7.11 (s, 1H, Ar–H), 7.32–7.39 (d, $J = 6.8$ Hz, 1H, Ar–H), 7.40–7.49 (m, 3H, Ar–H), 7.51–7.57 (m, 2H, Ar–H), 7.58–7.66 (m, 6H, Ar–H), 7.73 (s, 1H, Ar–H), 7.81 (d, $J = 8.3$ Hz, 2H, Ar–H); ^{13}C NMR (75 MHz, $CDCl_3$): δ 29.6, 50.0, 56.2, 56.3, 105.8, 107.6, 113.4, 120.4, 126.1, 126.8, 127.3, 127.4, 128.7, 128.9, 129.2, 130.1, 130.2, 130.3, 132.9, 136.3, 140.4, 140.8, 143.9, 147.7, 149.2, 152.4, 155.5, 161.2; ESI MS: $m/z = 530$ $[M+H]^+$; HRMS calculated for $C_{32}H_{28}N_5O_3$: 530.2114, Found: 530.2169.

*6.5.13. 6,7-Dimethoxy-2-methyl-3-(2-((4-(phenanthren-9-yl)-1H-1,2,3-triazol-1-yl)methyl)phenyl) quinazolin-4(3H)-one (**4m**)*

Yield 85%; mp 94–97 °C; IR (KBr) υ in cm^{-1}: 3010, 2935, 2849, 1668, 1508, 1395, 1256, 1028, 751; ^1H NMR (300 MHz, $CDCl_3$): δ 2.12 (s, 3H, CH_3), 3.93 (s, 3H, OCH_3), 3.96 (s, 3H, OCH_3), 5.40 (d, $J = 15.2$ Hz, $1H_a$, CH_2), 5.67 (d, $J = 15.2$ Hz, $1H_b$, CH_2), 7.10 (s, 1H, Ar–H), 7.53–7.73 (m, 9H, Ar–H), 7.79 (s, 1H, Ar–H), 7.90 (s, 2H, Ar–H), 8.34 (d, $J = 8.3$ Hz, 1H, Ar–H), 8.64–8.78 (m, 2H, Ar–H); ^{13}C NMR (75 MHz, $CDCl_3$): δ 29.6, 50.1, 56.2, 56.2, 105.7, 107.4, 113.3, 122.4, 122.6, 122.8, 123.5, 126.1, 126.5, 126.7, 126.8, 127.0, 127.6, 128.3, 128.5, 128.7, 128.9, 130.3, 131.1, 131.9, 132.0, 132.7, 132.8, 136.4, 143.7, 147.0, 149.0, 152.4, 155.4, 161.2; ESI MS: $m/z = 554$ $[M+H]^+$; HRMS calculated for $C_{34}H_{28}N_5O_3$: 554.2114, Found: 554.2171.

*6.5.14. 3-(2-((4-(Hydroxymethyl)-1H-1,2,3-triazol-1-yl)methyl) phenyl)-6,7-dimethoxy-2-methyl quinazolin-4(3H)-one (**4n**)*

Yield 85%; mp 105–108 °C; IR (KBr) υ in cm^{-1}: 2928, 1685, 1378, 1276, 1122, 776; ^1H NMR (300 MHz, $CDCl_3$): δ 2.00 (s, 3H, CH_3), 4.01 (s, 3H, OCH_3), 4.03 (s, 3H, OCH_3), 4.71 (s, 2H, CH_2), 5.23 (d, $J = 15.2$ Hz, $1H_a$, CH_2), 5.49 (d, $J = 15.2$ Hz, $1H_b$, CH_2), 7.12 (s, 1H, Ar–H), 7.20–7.25 (m, 1H, Ar–H), 7.35–7.42 (m, 1H, Ar–H), 7.48 (d, $J = 7.1$ Hz, 1H, Ar–H), 7.50–7.56 (m, 2H, Ar–H), 7.58 (s, 1H, Ar–H); ^{13}C NMR (75 MHz, $CDCl_3$): δ 29.6, 50.0, 55.5, 56.3, 56.4, 105.8, 107.4, 113.5, 123.9, 126.8, 128.9, 130.3, 132.8, 136.3, 139.5, 142.4, 143.8, 149.2, 152.6, 155.7, 161.1; ESI MS: $m/z = 408$ $[M+H]^+$; HRMS calculated for $C_{21}H_{22}N_5O_4$: 408.1594, Found: 408.1656.

*6.5.15. 3-(2-((4-(2-Hydroxyethyl)-1H-1,2,3-triazol-1-yl)methyl) phenyl)-6,7-dimethoxy-2-methyl quinazolin-4(3H)-one (**4o**)*

Yield 85%; mp 92–95 °C; IR (KBr) υ in cm^{-1}: 2928, 1683, 1378, 1276, 1126, 776; ^1H NMR (300 MHz, $CDCl_3$): δ 1.95 (s, 3H, CH_3), 2.74–3.01 (m, 2H, CH_2), 3.81–3.95 (m, 2H, CH_2), 4.00 (s, 3H, OCH_3), 4.03 (s, 3H, OCH_3), 5.36 (dd, $J = 12.4$, 15.1 Hz, 2H, CH_2), 7.12 (s, 1H, Ar–H), 7.20–7.25 (m, 1H, Ar–H), 7.34–7.40 (m, 1H, Ar–H), 7.48–7.65 (m, 4H, Ar–H); ^{13}C NMR (75 MHz, $CDCl_3$): δ 23.6, 29.0, 29.6, 56.3, 56.4, 71.7, 105.6, 106.6, 107.4, 116.3, 119.8, 123.3, 125.4, 128.5, 129.1, 130.3, 130.7, 131.0, 136.8, 145.7, 152.5, 166.5; ESI MS: $m/z = 422$ $[M+H]^+$; HRMS calculated for $C_{22}H_{24}N_5O_4$: 422.1750, Found: 422.1810.

*6.5.16. 3-(2-((4-(4-Methoxyphenyl)-1H-1,2,3-triazol-1-yl)methyl) phenyl)-2-methylquinazolin-4(3H)-one (**4p**)*

Yield 85%; mp 178–181 °C; IR (KBr) υ in cm^{-1}: 2928, 1728, 1682, 1470, 1378, 1276, 1123, 772; ^1H NMR (300 MHz, $CDCl_3$): δ 2.11 (s, 3H, CH_3), 3.84 (s, 3H, OCH_3), 5.27 (d, $J = 15.2$ Hz, $1H_a$, CH_2), 5.55 (d, $J = 15.2$ Hz, $1H_b$, CH_2), 6.93 (d, $J = 8.8$ Hz, 2H, Ar–H), 7.09–7.16 (m, 1H, Ar–H), 7.33–7.43 (m, 1H, Ar–H), 7.43–7.50 (m, 1H, Ar–H), 7.53 (s, 1H, Ar–H), 7.55 (d, $J = 3.3$ Hz, 1H, Ar–H), 7.61–7.76 (m, 4H, Ar–H), 7.79 (t, $J = 6.6$, 15.1 Hz, 1H, Ar–H), 8.31 (d, $J = 7.7$ Hz, 1H, Ar–H); ^{13}C NMR (75 MHz, $CDCl_3$): δ 29.5, 49.7, 55.3, 106.1, 110.6, 114.1, 119.5, 124.4, 127.0, 127.9, 128.7, 130.0, 130.4, 131.5, 132.9, 134.7, 135.0, 147.5, 148.1, 158.7, 162.9; ESI MS: $m/z = 424$ $[M+H]^+$; HRMS calculated for $C_{25}H_{22}O_2N_5$: 424.1768, Found: 424.1766.

*6.5.17. 2-Methyl-3-(2-((4-phenyl-1H-1,2,3-triazol-1-yl)methyl) phenyl)quinazolin-4(3H)-one (**4q**)*

Yield 85%; mp 91–94 °C; IR (KBr) υ in cm^{-1}: 2924, 2853, 1683, 1596, 1380, 1267, 1116, 767; ^1H NMR (300 MHz, $CDCl_3$): δ 2.12 (s, 3H, CH_3), 5.28 (d, $J = 15.1$ Hz, $1H_a$, CH_2), 5.57 (d, $J = 15.1$ Hz, $1H_b$, CH_2), 7.36–7.44 (m, 3H, Ar–H), 7.49–7.59 (m, 4H, Ar–H), 7.69–7.87 (m, 6H, Ar–H), 8.31 (d, $J = 9.2$ Hz, 1H, Ar–H); ^{13}C NMR (75 MHz, $CDCl_3$): δ 22.9, 46.3, 106.9, 111.5, 116.2, 119.8, 120.4, 124.3, 125.3, 125.7, 127.0, 128.1, 128.7, 130.1, 130.4, 130.9, 141.8, 144.2, 151.0, 156.2, 158.4, 163.7; ESI MS: $m/z = 394$ $[M+H]^+$; HRMS calculated for $C_{24}H_{20}0N_5$: 394.1662, Found: 394.1664.

*6.5.18. 3-(2-((4-(6-methoxynaphthalen-2-yl)-1H-1,2,3-triazol-1-yl)methyl)phenyl)-2-methylquinazolin-4(3H)-one (**4r**)*

Yield 85%; mp 188–191 °C; IR (KBr) υ in cm^{-1}: 3010, 2936, 2840, 1668, 1505, 1394, 1252, 1028, 753; ^1H NMR (300 MHz, $CDCl_3$): δ 2.26 (s, 3H, CH_3), 3.98 (s, 3H, OCH_3), 5.55 (d, $J = 15.1$ Hz, $1H_a$, CH_2), 5.81 (d, $J = 15.1$ Hz, $1H_b$, CH_2), 6.73–6.80 (m, 2H, Ar–H), 6.81–6.86 (m, 1H, Ar–H), 6.94–7.06 (m, 1H, Ar–H), 7.06–7.15 (m, 2H, Ar–H), 7.53–7.57 (m, 1H, Ar–H), 7.59 (bs, 2H, Ar–H), 7.68–7.77 (m, 1H, Ar–H), 7.80–7.99 (m, 1H, Ar–H), 8.09–8.13 (m, 1H, Ar–H), 8.22 (bs, 1H, Ar–H); ^{13}C NMR (75 MHz, $CDCl_3$): δ 23.6, 50.1, 55.2, 56.2, 56.3, 105.7, 105.8, 107.4, 113.4, 119.1, 120.3, 124.3, 125.4, 128.1, 127.1, 128.4, 128.8, 128.9, 129.6, 130.2, 130.3, 131.9, 132.9, 134.3, 136.3, 143.7, 148.2, 149.2, 152.6, 155.5, 157.9, 161.2; ESI MS: $m/z = 474$ $[M+H]^+$; HRMS calculated for $C_{29}H_{24}0_2N_5$: 474.1935, Found: 474.1928.

*6.6. General procedure for the synthesis of compounds (**4s**–**x**)*

To a stirred solution of compound **8a**–**b** (0.1 g, 0.306 mol) in toluene (15 ml), different triazoles (0.460 mol) and *p*TSA (10 mol%) were added at rt. The reaction mixture was refluxed for 36 h. After completion of the reaction, toluene was evaporated under vacuum. The obtained residue was dissolved in $CHCl_3$ (15 mL). The organic phase was washed with water (3 × 5 mL), separated, dried with Na_2SO_4, evaporated under reduced pressure and purified by column chromatography over silica gel (5:95, methanol/ethyl acetate) to afford **4s**–**x** as solid compounds.

*6.6.1. 3-(2-((1H-1,2,3-triazol-1-yl)methyl)phenyl)-6,7-dimethoxy-2-methylquinazolin-4(3H)-one (**4s**)*

Yield 78%; mp 87–90 °C; IR (KBr) υ in cm^{-1}: 2924, 2853, 1663, 1499, 1391, 1246, 1025, 747; ^1H NMR (300 MHz, $CDCl_3$): δ 2.03 (s, 3H, CH_3), 4.01 (s, 3H, OCH_3), 4.03 (s, 3H, OCH_3), 5.26 (d, $J = 15.2$ Hz, $1H_a$, CH_2), 5.55 (d, $J = 15.2$ Hz, $1H_b$, CH_2), 7.13 (s, 1H, Ar–H), 7.21–7.25 (m, 1H, Ar–H), 7.33–7.37 (m, 1H, Ar–H), 7.50–7.56 (m, 3H, Ar–H), 7.59 (s, 1H, Ar–H), 7.67 (d, $J = 0.9$ Hz, Ar–H); ^{13}C NMR (75 MHz, $CDCl_3$): δ 22.8, 38.9, 56.2, 56.2, 110.0, 112.8, 119.3, 125.4, 125.6, 127.4, 129.5, 130.9, 132.1, 133.5, 134.0, 146.0, 149.2, 152.9, 162.2, 166.4; ESI MS: $m/z = 378$ $[M+H]^+$; HRMS calculated for $C_{20}H_{20}0_3N_5$: 378.1560, Found: 378.1556.

*6.6.2. 3-(2-((4-Mercapto-1H-1,2,3-triazol-1-yl)methyl)phenyl)-6,7-dimethoxy-2-methyl quinazolin-4(3H)-one (**4t**)*

Yield 78%; mp 155–158 °C; IR (KBr) υ in cm^{-1}: 2925, 1669, 1500, 1393, 1250, 1028, 782; ^1H NMR (300 MHz, $CDCl_3$): δ 2.13 (s, 3H, CH_3), 3.99 (s, 3H, OCH_3), 4.04 (s, 3H, OCH_3), 4.25 (d, $J = 12.7$ Hz, $1H_a$, CH_2), 4.44 (d, $J = 12.7$ Hz, $1H_b$, CH_2), 7.19 (s, 1H, Ar–H), 7.44 (t, $J = 7.4$, 12.8 Hz, 1H, Ar–H), 7.50–7.60 (m, 4H, Ar–H), 8.35 (d, $J = 9.5$ Hz, Ar–H); ^{13}C NMR (75 MHz, $CDCl_3$): δ 24.2, 32.7, 56.0, 56.2, 122.3, 126.6, 126.9, 127.6, 128.0, 129.2, 130.1, 131.2, 134.6, 136.0, 136.1, 142.3, 154.4, 161.3; ESI MS: $m/z = 410$ $[M+H]^+$; HRMS calculated for $C_{26}H_{24}N_50_3$: 410.1210, Found: 410.1312.

*6.6.3. 3-(2-((1H-[1,2,3]triazolo[4,5-b]pyridin-1-yl)methyl)phenyl)-6,7-dimethoxy-2-methyl quinazolin-4(3H)-one (**4u**)*

Yield 78%; mp 215–218 °C; IR (KBr) υ in cm^{-1}: 3010, 2934, 2838, 1668, 1496, 1392, 1248, 1027, 752; ^1H NMR (300 MHz, $CDCl_3$): δ 1.86 (s, 3H, CH_3), 4.03 (s, 6H, $2OCH_3$), 5.80 (dd, $J = 12.8$, 15.1 Hz, 2H, CH_2), 7.05 (s, 1H, Ar–H), 7.17–7.26 (m, 2H, Ar–H), 7.49–7.56 (m, 2H, Ar–H), 7.61–7.68 (m, 2H, Ar–H), 8.30–8.37 (m, 2H, Ar–H); ^{13}C NMR (75 MHz, $CDCl_3$): δ 23.5, 46.3, 56.0, 56.2, 105.9, 107.3, 113.9, 119.8, 128.4, 128.8, 129.9, 130.1, 131.0, 133.1, 136.4, 136.6, 143.7, 145.4, 148.9, 150.2, 152.5, 155.1, 161.2; ESI MS: $m/z = 429$ $[M+H]^+$; HRMS calculated for $C_{23}H_{21}0_3N_6$: 429.1669, Found: 429.1654.

*6.6.4. 3-(2-((1H-1,2,3-triazol-1-yl)methyl)phenyl)-2-methylquinazolin-4(3H)-one (**4v**)*

Yield 78%; mp 88–91 °C; IR (KBr) υ in cm^{-1}: 2917, 2247, 2126, 1621, 1380, 1219, 1020, 771; ^1H NMR (300 MHz, $CDCl_3$): δ 2.09 (s, 3H, CH_3), 4.16 (s, 2H, CH_2), 6.36 (d, $J = 9.0$ Hz, 1H, Ar–H), 7.04 (t, $J = 8.0$, 16.0 Hz, 1H, Ar–H), 7.31–7.41 (m, 3H, Ar–H), 7.43–7.47 (m, 1H, Ar–H), 7.55 (s, 1H, Ar–H), 7.67 (s, 1H, Ar–H), 7.74 (d, $J = 8.0$ Hz, 1H, Ar–H), 8.12 (d, $J = 9.0$ Hz, 1H, Ar–H); ^{13}C NMR (75 MHz, $CDCl_3$): δ 22.8, 38.9, 110.0, 113.8, 119.3, 125.4, 125.6, 127.4, 128.5, 130.9, 133.1, 133.5, 135.0, 146.4, 149.4, 152.9, 160.2, 169.4; ESI MS: $m/z = 318$ $[M+H]^+$; HRMS calculated for $C_{18}H_{16}N_50$: 318.1277, Found: 318.1309.

*6.6.5. 3-(2-((4-Mercapto-1H-1,2,3-triazol-1-yl)methyl)phenyl)-2-methylquinazolin-4(3H)-one (**4w**)*

Yield 78%; mp 142–143 °C; IR (KBr) υ in cm^{-1}: 2923, 1600, 1471, 1382, 1219, 1120, 772; ^1H NMR (400 MHz, $CDCl_3$): δ 2.36 (s, 3H, CH_3), 4.03 (d, $J = 13.9$ Hz, $1H_a$, CH_2), 4.19 (d, $J = 13.9$ Hz, $1H_b$, CH_2), 7.21 (d, $J = 8.3$ Hz, 1H, Ar–H), 7.26 (s, 1H, Ar–H), 7.34–7.48 (m, 2H, Ar–H), 7.48 (t, $J = 7.4$, 14.8 Hz, 1H, Ar–H), 7.71 (d, $J = 7.4$ Hz, 1H, Ar–H), 7.79 (t, $J = 7.4$, 14.8 Hz, 1H, Ar–H), 7.89 (s, 1H, Ar–H), 8.30 (d, $J = 7.4$ Hz, 1H, Ar–H); ^{13}C NMR (75 MHz, $CDCl_3$): δ 24.1, 32.7, 120.3, 126.6, 126.9, 127.1, 128.7, 129.4, 130.0, 131.2, 134.6, 135.0, 136.1, 147.3, 154.4, 162.3; ESI MS: $m/z = 350$ $[M+H]^+$; HRMS calculated for $C_{18}H_{16}0N_5S$: 350.1070, Found: 350.1065.

*6.6.6. 3-(2-((1H-[1,2,3]triazolo[4,5-b]pyridin-1-yl)methyl)phenyl)-2-methylquinazolin -4(3H)-one (**4x**)*

Yield 78%; mp 210–213 °C; IR (KBr) υ in cm^{-1}: 2924, 2853, 1682, 1462, 1380, 1275, 1075, 772; ^1H NMR (300 MHz, $CDCl_3$): δ 2.11 (s, 3H, CH_3), 5.56 (d, $J = 15.8$ Hz, $1H_a$, CH_2), 5.88 (d, $J = 15.8$ Hz, $1H_b$, CH_2), 7.12 (d, $J = 7.5$ Hz, 1H, Ar–H), 7.31 (s, 1H, Ar–H), 7.43–7.59 (m, 3H, Ar–H), 7.69 (d, $J = 7.5$ Hz, 1H, Ar–H), 7.80 (d, $J = 1.5$ Hz, 1H, Ar–H), 7.82–7.85 (m, 1H, Ar–H), 7.87 (d, $J = 1.5$ Hz, 1H, Ar–H), 8.29–8.33 (m, 1H, Ar–H), 8.72 (dd, $J = 1.5$, 4.5 Hz, 1H, Ar–H); ^{13}C NMR (75 MHz, $CDCl_3$): δ 26.7, 48.5, 104.9, 110.0, 119.0, 122.4, 124.6, 126.2, 126.9, 127.1, 128.9, 129.2, 130.3, 130.4, 132.3, 135.1, 147.5, 148.4, 153.5, 158.9; ESI MS: $m/z = 369$ $[M+H]^+$; HRMS calculated for $C_{21}H_{17}0N_6$: 369.1458, Found: 369.1458.

6.7. Biological methods

6.7.1. Cell culture

MCF-7 (human breast cancer), HeLa (human cervical cancer) and K562 (human leukemia) cells were cultured by using Dulbecco's modified Eagle's medium (DMEM), supplemented with 10% fatal calf serum, 100 μg/mL penicillin-G and 100 μg/mL streptomycin sulfate (Sigma) followed by incubation at 37 °C in a humidified atmosphere containing 5% CO_2 in the incubator.

6.7.2. Assessment of cell viability by MTT assay

Cell viability was assessed by the MTT assay using Vibrant MTT based cell proliferation assay kit (Invitrogen), which is based on the

ability of viable cells to reduce the MTT to insoluble Formosan crystals by mitochondrial dehydrogenase. Individual wells of a 96-well tissue culture microtiter plate were inoculated with 100 μL of complete medium containing 1 10^4 cells (MCF-7, HeLa and K562 cells). The plates were incubated at 37 °C in a humidified 5% CO_2 incubator for 18 h prior to the experiment. After medium removal, 100 μL of fresh medium containing the test compounds at varying concentration ranging from 1 to 256 μM concentration was added and incubated at 37 °C for 72 h. Then the medium was discarded and replaced with 10 μL MTT dye. Plates were incubated at 37 °C for 2 h. The resulting formazan crystals were solubilized in 100 μL extraction buffer. The optical density (O.D.) was read at 570 nm with micro plate reader. The percentage of DMSO in the medium never exceeded 0.25%.

6.7.3. Flow cytometric analysis of cell cycle distribution

For flow cytometric analysis of DNA content, 5 10^5 HeLa cells in exponential phase of growth were treated at a concentration of 2 μM of compounds (**Luotonin A**, **4q**, **4r**, **4e**, **4k**, **4t** and **4w**) for 24 h. After the incubation period, the cells were collected, centrifuged and fixed with ice-cold 70% ethanol at 4 °C for 30 min. Then the cells were incubated with 1 mg/ml RNAase A solution (Sigma) at 37 °C for 30 min followed by staining with 250 μL of DNA staining solution [10 mg of Propidium Iodide (PI), 0.1 mg of trisodium citrate, and 0.03 mL of Triton X-100 dissolved in 100 mL of sterile MilliQ water at room temperature for 30 min in the dark]. The DNA contents of 20,000 events were measured by flow cytometer (DAKO CYTOMATION, Beckman Coulter, Brea, CA). Histograms were analyzed using Summit Software.

6.7.4. X-gal staining for senescence associated β-gal assay

The activity of endogenous β-galactosidase, an important biomarker for cells undergoing senescence was used to detect any senescent cells. Here, HeLa cells were taken at a density of 0.1 10^5 in chamber slide. Treatments were carried out with effective compound (**4q**) along with standard **Doxo** and **Luotonin A** for 72 h at 4 μM concentration. Cells were fixed in 3% para-formaldehyde and then incubated for 10 min at room temperature. After thorough PBS wash the cells were again fixed in methanol for 20 min at 4 °C. This is followed by incubation in sodium phosphate buffer containing 2 mg X-gal, $K_4Fe(CN)_6.3H_20$, $K_3Fe(CN)_6$,1 mM $MgCl_2$, 2 M NaCl, 0.1 M citric acid for 24 h. The Cells were then subjected to microscopy studies for visualization of blue color formation, which is a clear indication of cells undergoing senescence.

6.7.5. Semi-quantitative reverse transcription PCR (RT-PCR)

Total RNA was extracted using RNeasy mini kit (Qiagen, USA) and reverse transcribed into cDNA using superscript II reverse transcriptase (Invitrogen life technologies). PCR was carried out with specific primers against p53, p21, EZH2 and HDAC-1,2,5,6,7 genes in PCR (Takara, Bioscience) machine. GAPDH was used as a loading control. The products were electrophoresed on agarose gel (1%) followed by staining with ethidium bromide and visualized under U.V. light. The signal intensity of respective bands was measured by means of the quantity one version 4.1.1 software using BIORAD image analysis system (CA, USA).

6.7.6. HDAC-1/2 assay

The HDAC-1 and 2 calorimetric assay is based on the unique Color de lys substrate and developer combination. Here the compound and TSA treated cells (at 4 μM) were incubated with the de Color lys substrate and HDAC-1 and 2 (BML-K 1137) for 30 min to observe the inhibitory activity of compounds on HDAC-1 and 2 proteins. The deacetylation of substrate sensitizes the substrate and developer produces yellow color which has an absorption maxima at 405 nm (**Enzo Life Sciences USA**). These colorimetric readings were recorded using Multimode varioskan instrument (**Thermo scientific, USA**).

6.7.7. Cloning and transfection assay

Luciferase enzyme based transfection assays were carried out since luciferase serves as reporter for the promoter activation. The p16 promoter (1.4 Kb) was cloned in Luciferase based reporter vector pGL3 basic. Here the promoter construct as well as β-gal plasmid were co-transfected in HeLa cells followed by treatment with **4q**, **Doxo** and **Luotonin A** at 4 μM for 48 h. The lysates were subjected to luciferase based assay using varioskan Flash (Thermo Scientific) and values were plotted in the form of graph with β-galactosidase being used as an internal control.

6.8. Computational methods

6.8.1. Dataset preparation

A dataset comprising a series of 24 quinazolinone hybrids and its inhibitory data (IC_{50} μM) were obtained from MTT based cytotoxicity assay. These series of compounds were converted into 3D-molecules with all possible tautomers and chiral centers. The converted 3D-molecules were minimized with OPLS-2005 force field using water as solvent in the GB/SA continuum solvation model [63] distance dependent electrostatic treatment was done at dielectric constant of 1.0; and the cutoff for potential energy calculation was kept extended. The extended cutoff includes contribution of van der Waals (8.0), electrostatic (20) and hydrogen bond (4.0) interactions. The minimization of molecules was carried out using Polak–Ribiere Conjugate Gradient (PRCG) method with maximum of 5000 iterations. The minimized compounds were used for molecular docking study.

6.8.2. Pharmacophore modeling

The pharmacophore model was generated using Phase module of Schrödinger software v9.3. The set of pharmacophore features, such as hydrogen bond acceptor (A), hydrogen bond donor (D), hydrophobic group (H), negatively ionizable (N), positively ionizable (P), and aromatic ring (R), were created for a series of compounds containing MCF-7 cell-line activity. The best common pharmacophore hypothesis has been selected among the generated pharmacophore hypotheses using the conformations of a series of 24 compounds. The selection of common pharmacophore depends on the *alignment score* (based on root mean squared deviation), *vector score* (based on average cosine angles between acceptors, donors and aromatic rings), and *volume score* (based on van der Waals volume).

6.8.3. Homology modeling

For the present study, the human HDAC5 and HDAC6 homology models were built, using human HDAC2 (PDB ID: 3MAX) as a template by using Prime module of Schrödinger software version 9.3. The catalytic domain of HDAC2 showed 16%, 20% identity and 30%, 35% similarity with HDAC5 (residues from 596 to 1120), HDAC6 (477–875) catalytic subunits respectively. The pairwise alignment between HDACs was done with inbuilt BLAST [64] and ClustalW [65] algorithms. Further, for building HDAC homology models, energy-based method was used to retain rotamers for conserved residues, optimize the side chains, minimize residues not derived from templates and omit the template gaps more than 20 residues. The active site information for EZH2 is unknown. We identified active site pockets and its key active site residues using mutagenesis data [66–68] and sitemap analysis in Maestro software.

6.8.4. Protein preparation

The crystal structure of HDAC proteins i.e HDAC1 (PDB ID: 4BKX), HDAC2 (PDB ID: 3MAX) and HDAC7 (PDB ID: 3ZNR), its homology models i.e HDAC5 (Uniprot ID: Q9UQL6), HDAC6 (Uniprot ID: Q9UBN7) and EZH2 (histone-lysine N-methyltransferase, PDB ID: 4MI0) have been selected for the docking studies. The protein structures were prepared by adjusting bond orders, tautomers and adding hydrogen atoms using protein preparation wizard of Schrödinger software graphical user interface Maestro v9.3. Further the proteins were minimized by OPLS_2005 force field with converge heavy atoms to RMSD 0.3 Å relative to original protein structures.

6.8.5. Docking studies

The docking study has been carried out on a series of minimized quinazolinone series of compounds with prepared proteins using Schrödinger docking program module [69]. The prepared protein structures (4BKX, 3MAX, 3ZNR, 4MI0 complexes and HDAC5, HDAC6 models) were used for grid generation. No constraints were imposed and extraprecision (XP) docking of ligands was used. The obtained docked complex structures were analyzed and compounds were prioritized by using docking score, interactions with active site residues.

Acknowledgments

The authors gratefully acknowledge DST-SERB/EMEQ-078/2013 and DENOVA (CSC0205) New Delhi for financial assistance and RV thanks CSIR, New Delhi for award of research fellowship.

Appendix A. Supplementary data

Supplementary data related to this article can be found at http://dx.doi.org/10.1016/j.ejmech.2015.02.057.

References

[1] M. Viale, M.A. Mariggio, M. Ottone, B. Chiavarina, A. Vinella, C. Prevosto, C. Dell'Erba, G. Petrillo, M. Novi, Invest. New. Drugs 22 (2004) 359–367.
[2] S. Minucci, P.G. Pelicci, Nat. Rev. Cancer 6 (2006) 38–51.
[3] A.J. de Ruijter, A.H. van Gennip, H.N. Caron, S. Kemp, A.B. van Kuilenburg, Biochem. J. 370 (2003) 737–749.
[4] G. Giannini, W. Cabri, C. Fattorusso, M. Rodriquez, Future Med. Chem. 4 (2012) 1439–1460.
[5] R.C. Trievel, Crit. Rev. Eukaryot. Gene Expr. 14 (2004) 147–169.
[6] J. Baxter, S. Sauer, A. Peters, R. John, R. Williams, M.L. Caparros, K. Arney, A. Otte, T. Jenuwein, M. Merkenschlager, A.G. Fisher, EMBO J. 23 (2004) 4462–4472.
[7] Y. Yuan, Q. Wang, J. Paulk, S. Kubicek, M.M. Kemp, D.J. Adams, A.F. Shamji, B.K. Wagner, S.L. Schreiber, ACS Chem. Biol. 7 (2012) 1152–1157.
[8] W. Fiskus, M. Pranpat, M. Balasis, B. Herger, R. Rao, A. Chinnaiyan, P. Atadja, K. Bhalla, Mol. Cancer Ther. 5 (2006) 3096–3104.
[9] J. Yamaguchi, M. Sasaki, Y. Sato, K. Itatsu, K. Harada, Y. Zen, H. Ikeda, Y. Nimura, M. Nagino, Y. Nakanuma, Cancer Sci. 101 (2010) 355–362.
[10] J.M. Klein, A. Henke, M. Sauer, M. Bessler, K.S. Reiners, A. Engert, H.P. Hansen, E.P. von Strandmann, PLoS One 8 (2013) e79502.
[11] M.J. Chuang, S.T. Wu, S.H. Tang, X.M. Lai, H.C. Lai, K.H. Hsu, K.H. Sun, G.H. Sun, S.Y. Chang, D.S. Yu, P.W. Hsiao, S.M. Huang, T.L. Cha, PLoS One 8 (2013) e73401.
[12] W. Song, Y.T. Tai, Z. Tian, T. Hideshima, D. Chauhan, P. Nanjappa, M.A. Exley, K.C. Anderson, N.C. Munshi, Leukemia 25 (2011) 161–168.
[13] A.A. Lane, B.A. Chabner, J. Clin. Oncol. 27 (2009) 5459–5468.
[14] J.S. Carew, F.J. Giles, S.T. Nawrocki, Cancer Lett. 269 (2008) 7–17.
[15] W.S. Xu, R.B. Parmigiani, P.A. Marks, Oncogene 26 (2007) 5541–5552.
[16] M. Paris, M. Porcelloni, M. Binaschi, D. Fattori, J. Med. Chem. 51 (2008) 1505–1529.
[17] K. Harms, S. Nozell, X. Chen, Cell. Mol. Life Sci. 61 (2004) 822–842.
[18] J. Bartkova, N. Rezaei, M. Liontos, P. Karakaidos, D. Kletsas, N. Issaeva, L.V. Vassiliou, E. Kolettas, K. Niforou, V.C. Zoumpourlis, M. Takaoka, H. Nakagawa, F. Tort, K. Fugger, F. Johansson, M. Sehested, C.L. Andersen, L. Dyrskjot, T. Orntoft, J. Lukas, C. Kittas, T. Helleday, T.D. Halazonetis, J. Bartek, V.G. Gorgoulis, Nature 444 (2006) 633–637.
[19] V.L. Gabai, C. O'Callaghan-Sunol, L. Meng, M.Y. Sherman, J. Yaglom, Cancer Res. 68 (2008) 1834–1842.
[20] R.F. Place, E.J. Noonan, C. Giardina, Biochem. Pharmacol. 70 (2005) 394–406.
[21] M. Wagner, G. Brosch, W. Zwerschke, E. Seto, P. Loidl, P. Jansen-Durr, FEBS Lett. 499 (2001) 101–106.
[22] J.W. Jung, S. Lee, M.S. Seo, S.B. Park, A. Kurtz, S.K. Kang, K.S. Kang, Cell. Mol. Life Sci. 67 (2010) 1165–1176.
[23] K. Okumura, T. Oine, Y. Yamada, G. Hayashi, M. Nakama, J. Med. Chem. 11 (1968) 348–352.
[24] G. Bonola, P. Da Re, M.J. Magistretti, E. Massarani, I. Setnikar, J. Med. Chem. 11 (1968) 1136–1139.
[25] S.L. Gackenheimer, J.M. Schaus, D.R. Gehlert, J. Pharmacol. Exp. Ther. 274 (1995) 1558–1565.
[26] R.O. Dempcy, E.B. Skibo, Biochemistry (Mosc.) 30 (1991) 8480–8487.
[27] J.P. Michael, Nat. Prod. Rep. 22 (2005) 627–646.
[28] A. Elkamhawy, J. Lee, B.G. Park, I. Park, A.N. Pae, E.J. Roh, Eur. J. Med. Chem. 84 (2014) 466–475.
[29] M.L. Barbosa, L.M. Lima, R. Tesch, C.M. Sant'Anna, F. Totzke, M.H. Kubbutat, C. Schächtele, S.A. Laufer, E.J. Barreiro, Eur. J. Med. Chem. 71 (2014) 1–14.
[30] Y. Zhang, Y.J. Huang, H.M. Xiang, P.Y. Wang, D.Y. Hu, W. Xue, B.A. Song, S. Yang, Eur. J. Med. Chem. 78 (2014) 23–34.
[31] L.B. Saltz, J.V. Cox, C. Blanke, L.S. Rosen, L. Fehrenbacher, M.J. Moore, J.A. Maroun, S.P. Ackland, P.K. Locker, N. Pirotta, G.L. Elfring, L.L. Miller, N. Engl. J. Med. 343 (2000) 905–914.
[32] C.H. Takimoto, J. Wright, S.G. Arbuck, Biochim. Biophys. Acta 1400 (1998) 107–119.
[33] U. Vanhoefer, A. Harstrick, W. Achterrath, S. Cao, S. Seeber, Y.M. Rustum, J. Clin. Oncol. 19 (2001) 1501–1518.
[34] A. Cagir, S.H. Jones, R. Gao, B.M. Eisenhauer, S.M. Hecht, J. Am. Chem. Soc. 125 (2003) 13628–13629.
[35] A. Cagir, B.M. Eisenhauer, R. Gao, S.J. Thomas, S.M. Hecht, Bioorg. Med. Chem. 12 (2004) 6287–6299.
[36] W. Guerrant, V. Patil, J.C. Canzoneri, A.K. Oyelere, J. Med. Chem. 55 (2012) 1465–1477.
[37] N. Humbert, S. Martien, A. Augert, M. Da Costa, S. Mauen, C. Abbadie, Y. De Launoit, J. Gil, D. Bernard, Cancer Res. 69 (2009) 410.
[38] Q. Zhou, Y. Wang, L. Yang, Y. Wang, P. Chen, Y. Wang, X. Dong, L. Xie, Mol. Vis. 14 (2008) 2556–2565.
[39] M.G. Ferlin, R. Bortolozzi, P. Brun, I. Castagliuolo, E. Hamel, G. Basso, G. Viola, ChemMedChem 5 (2010) 1373–1385.
[40] L.D. Via, O. Gia, V. Gasparotto, M.G. Ferlin, Eur. J. Med. Chem. 43 (2008) 429–434.
[41] L. Nagarapu, H.K. Gaikwad, R. Bantu, S.R. Manikonda, Eur. J. Med. Chem. 46 (2011) 2152–2156.
[42] L. Nagarapu, H.K. Gaikwad, K. Sarikonda, J. Mateti, R. Bantu, P.S. Raghu, K.M. Manda, S.V. Kalvendi, Eur. J. Med. Chem. 45 (2010) 4720–4725.
[43] L. Nagarapu, V. Paparaju, A. Satyender, Bioorg. Med. Chem. Lett. 18 (2008) 2351–2354.
[44] B. Yadagiri, U.D. Holagunda, R. Bantu, L. Nagarapu, C.G. Kumar, S.U. Pombala, B. Sridhar, Eur. J. Med. Chem. 79 (2014) 260–265.
[45] S. Janardhan, P. Srivani, G.N. Sastry, QSAR Comb. Sci. 25 (2006) 860–872.
[46] S. Janardhan, P. Srivani, G.N. Sastry, Curr. Med. Chem. 13 (2006) 1169–1186.
[47] P. Badrinarayan, G.N. Sastry, Comb. Chem. High. Throughput Screen 14 (2011) 840–860.
[48] A.S. Reddy, S.P. Pati, P.P. Kumar, H.N. Pradeep, G.N. Sastry, Curr. Protein Pept. Sci. 8 (2007) 329–351.
[49] F. Hoppe-Seyler, K. Butz, J. Virol. 67 (1993) 3111–3117.
[50] J.C. Law, M.K. Ritke, J.C. Yalowich, G.H. Leder, R.E. Ferrell, Leuk. Res. 17 (1993) 1045–1050.
[51] M. Fallahi-Sichani, S. Honarnejad, L.M. Heiser, J.W. Gray, P.K. Sorger, Nat. Chem. Biol. 9 (2013) 708–714.
[52] J. Campisi, F. d'Adda di Fagagna, Nat. Rev. Mol. Cell. Biol. 8 (2007) 729–740.
[53] M. Collado, M. Serrano, Nat. Rev. Cancer 10 (2010) 51–57.
[54] C.A. Afshari, P.J. Vojta, L.A. Annab, P.A. Futreal, T.B. Willard, J.C. Barrett, Exp. Cell. Res. 209 (1993) 231–237.
[55] E. Michishita, K. Nakabayashi, H. Ogino, T. Suzuki, M. Fujii, D. Ayusawa, Biochem. Biophys. Res. Commun. 253 (1998) 667–671.
[56] R. Di Micco, M. Fumagalli, A. Cicalese, S. Piccinin, P. Gasparini, C. Luise, C. Schurra, M. Garre, P.G. Nuciforo, A. Bensimon, R. Maestro, P.G. Pelicci, F. d'Adda di Fagagna, Nature 444 (2006) 638–642.
[57] A. Rebbaa, X. Zheng, P.M. Chou, B.L. Mirkin, Oncogene 22 (2003) 2805–2811.
[58] G.P. Dimri, X. Lee, G. Basile, M. Acosta, G. Scott, C. Roskelley, E.E. Medrano, M. Linskens, I. Rubelj, O. Pereira-Smith, et al., Proc. Natl. Acad. Sci. U. S. A. 92 (1995) 9363–9367.
[59] A.J. Levine, p53, Cell 88 (1997) 323–331.
[60] Y. Tang, W. Zhao, Y. Chen, Y. Zhao, W. Gu, Cell 133 (2008) 612–626.
[61] S. Janardhan, Y. Padmanabha Reddy, Int. J. Pharma. Res. Dev. 2 (2011) 131–146.
[62] C.S. Reddy, K. Vijayasarathy, E. Srinivas, G.M. Sastry, G.N. Sastry, Comput. Biol. Chem. 30 (2006) 120–126.
[63] A. Cheng, S.A. Best, K.M. Merz Jr., C.H. Reynolds, J. Mol. Graph. Model. 18 (2000) 273–282.
[64] S.B. Needleman, C.D. Wunsch, J. Mol. Biol. 48 (1970) 443–453.
[65] J.D. Thompson, D.G. Higgins, T.J. Gibson, Nucleic Acids Res. 22 (1994) 4673–4680.
[66] T.L. Cha, B.P. Zhou, W. Xia, Y. Wu, C.C. Yang, C.T. Chen, B. Ping, A.P. Otte,

M.C. Hung, Science 310 (2005) 306–310.
[67] S. Chen, L.R. Bohrer, A.N. Rai, Y. Pan, L. Gan, X. Zhou, A. Bagchi, J.A. Simon, H. Huang, Nat. Cell. Biol. 12 (2010) 1108–1114.
[68] A. Kuzmichev, K. Nishioka, H. Erdjument-Bromage, P. Tempst, D. Reinberg, Genes. Dev. 16 (2002) 2893–2905.
[69] R.A. Friesner, J.L. Banks, R.B. Murphy, T.A. Halgren, J.J. Klicic, D.T. Mainz, M.P. Repasky, E.H. Knoll, M. Shelley, J.K. Perry, D.E. Shaw, P. Francis, P.S. Shenkin, J. Med. Chem. 47 (2004) 1739–1749.